

P-wave heavy quarkonium spectrum with next-to-next-to-next-to-leading logarithmic accuracy

Clara Peset^{*}

*Physik Department T31, James-Franck-Straße 1, Technische Universität München,
85748 Garching, Germany*

Antonio Pineda[†] and Jorge Segovia[‡]

*Grup de Física Teòrica, Departament Física and IFAE-BIST, Universitat Autònoma de Barcelona,
E-08193 Bellaterra (Barcelona), Spain*



(Received 5 September 2018; published 8 November 2018)

We compute the heavy quarkonium mass of $l \neq 0$ (angular momentum) states, with otherwise arbitrary quantum numbers, with next-next-to-next-to-leading logarithmic (N^3LL) accuracy. This constitutes the first observable in heavy quarkonium for which two orders of the weak-coupling expansion sensitive to the ultrasoft scale are known and the resummation of ultrasoft logarithms is made. We also obtain, for the first time, resummed N^3LL expressions for the different fine and hyperfine energy splittings of these states, which are not sensitive to the ultrasoft scale but still require resummation of (hard) logarithms. We do this analysis for the equal and non-equal mass cases. We also study an alternative computational scheme that treats the static potential exactly. We then perform a comprehensive phenomenological analysis: we apply these results to the $n = 2$, $l = 1$ bottomonium, B_c and charmonium systems and study their convergence.

DOI: [10.1103/PhysRevD.98.094003](https://doi.org/10.1103/PhysRevD.98.094003)

I. INTRODUCTION

The heavy quarkonium mass has been computed with increasing accuracy in the limit of very large mass (i.e., in the strict weak-coupling approximation) over the years. If n represents the principal quantum number and l the orbital angular momentum, in this paper we exclusively consider non- S -wave states (i.e., those states with $l \neq 0$). Typically, we will use the notation “ P -wave” to refer to non- S -wave states (unless explicitly stated otherwise). The heavy quarkonium mass of the P -wave states has been computed in Ref. [1] to next-to-leading order (NLO), in Ref. [2] to NNLO, in Ref. [3] the $\ln \alpha_s$ term of the N^3LO , in Refs. [4,5] with N^3LO accuracy for the equal mass case and in Ref. [6] for the nonequal mass case. For the $n = 2$ and $l = 1$ fine splitting in the equal mass case, the N^3LO expression was obtained in Ref. [7] and the hyperfine in Ref. [8] (for arbitrary quantum numbers and equal masses).

Once the spectrum has been obtained with N^3LO accuracy, one can move to the next step: the computation of the heavy quarkonium mass with N^3LL accuracy by the resummation of the large logarithms. This is one of the main purposes of this paper, and we achieve this goal for arbitrary P -wave states. Most of the necessary ingredients are already available in the literature. The ultrasoft renormalization group (RG) analysis of the potentials relevant for the P -wave states were obtained with N^3LL accuracy in Ref. [9]. These results, together with the detailed computations in Ref. [6], allow us to obtain the mass of the excited states with N^3LL accuracy. We also achieve this precision for the fine and hyperfine P -wave splittings for the first time. Crucial to obtain this last result is the knowledge of the potential to N^3LO , of the structure of the potential in terms of Wilson loops, and the confirmation that no ultrasoft effects enter at this order. The above results are obtained using the effective field theory (EFT) named potential nonrelativistic QCD (pNRQCD) [10,11] (for reviews see [12,13]).

The cancellation of the leading renormalon of the pole mass and the static potential, first found in Ref. [14], and later in [15,16], led to the realization [16] that using threshold masses [16–20] (which explicitly implement the cancellation of the renormalon in heavy quarkonium observables) improves the convergence of the perturbative

^{*} clara.peset@tum.de

[†] pineda@ifae.es

[‡] jsegovia@ifae.es

Published by the American Physical Society under the terms of the Creative Commons Attribution 4.0 International license. Further distribution of this work must maintain attribution to the author(s) and the published article's title, journal citation, and DOI. Funded by SCOAP³.

series. This makes these very precise computations useful not only for academical purposes but also for phenomenological applications. The applicability of a weak-coupling analysis to the first P -wave heavy quarkonium excited state ($n = 2$, $l = 1$) is an open issue. Originally, they were studied in Refs. [21–24], where the outcome of the analysis was qualitatively positive. These analyses had NNLO accuracy and used the Upsilon counting [25], which effectively introduces the cancellation of renormalon but does not use threshold masses. An analysis of the fine splittings, which are directly renormalon free, was done in Ref. [7]. Beyond NNLO there is only a preliminary phenomenological analysis in N³LO using the Upsilon counting [4] and the more recent analysis [26].

On the phenomenological side, one of the purposes of this paper is to study the P -wave states of heavy quarkonium for bottomonium, charmonium and B_c (but specially bottomonium) to clarify if a weak-coupling description for them is appropriate, and, if so, to which extent. Nonperturbative corrections are parametrically smaller than the perturbative terms we neglect, and depend on how one treats the perturbative expansion. Therefore, we refrain of incorporating nonperturbative effects until we get a more clear understanding of the asymptotic behavior of the perturbative series. Actually, this is one of the reasons we do a strict perturbative analysis in this paper: We believe it is important to study pure perturbative predictions before start including nonperturbative effects. We also study separately the effect of the pure ultrasoft contributions, when they appear, as those contributions are the ones expected to be more sensitive to nonperturbative dynamics. The threshold mass we will use is the RS' mass [18]. We also want to quantify the impact of the resummation of logarithms in the heavy quarkonium spectrum: for the first time we have two terms of the weak-coupling expansion that depend on the ultrasoft logarithmic resummation.

Besides the aforementioned phenomenological analysis performed at strict weak coupling, we also study the convergence of an alternative computational scheme that reorganizes the perturbative expansion of the weak-coupling computation. This scheme is characterized by solving the Schrödinger equation including the static potential exactly (to the order it is known). This incorporates formally subleading terms in the leading-order (LO) solution. On the other hand the relativistic corrections to the spectrum are included perturbatively. This working scheme performs a partial resummation of higher-order effects. This may accelerate the convergence of the perturbative series. This is indeed the effect seen in (most of) the cases where it has been applied (spectrum and decays) [23,24,27,28] (the acceleration is somewhat more marginal in the analysis in Ref. [29]). This scheme naturally leads to the organization of the computation in powers of v , the relative velocity of the heavy quark in the bound state.

A. pNRQCD

Integrating out the soft modes in NRQCD [30,31], we obtain the EFT named pNRQCD [10]. The most general pNRQCD Lagrangian compatible with the symmetries of QCD that can be constructed with a singlet and an octet (quarkonium) fields, as well as an ultrasoft gluon field to NLO in the multipole expansion has the form [10,11]

$$\begin{aligned} \mathcal{L}_{\text{pNRQCD}} = & \int d^3\mathbf{r} \text{Tr} \{ S^\dagger (i\partial_0 - h_s(\mathbf{r}, \mathbf{p}, \mathbf{P}_R, \mathbf{S}_1, \mathbf{S}_2)) S \\ & + O^\dagger (iD_0 - h_o(\mathbf{r}, \mathbf{p}, \mathbf{P}_R, \mathbf{S}_1, \mathbf{S}_2)) O \} \\ & + V_A(r) \text{Tr} \{ O^\dagger \mathbf{r} \cdot g\mathbf{E}S + S^\dagger \mathbf{r} \cdot g\mathbf{E}O \} \\ & + \frac{V_B(r)}{2} \text{Tr} \{ O^\dagger \mathbf{r} \cdot g\mathbf{E}O + O^\dagger O \mathbf{r} \cdot g\mathbf{E} \} \\ & - \frac{1}{4} G_{\mu\nu}^a G^{\mu\nu a} + \sum_{i=1}^{n_f} \bar{q}_i i \not{D} q_i, \end{aligned} \quad (1.1)$$

$$h_s(\mathbf{r}, \mathbf{p}, \mathbf{P}_R, \mathbf{S}_1, \mathbf{S}_2) = \frac{\mathbf{p}^2}{2m_r} + \frac{\mathbf{P}_R^2}{2M} + V_s(\mathbf{r}, \mathbf{p}, \mathbf{P}_R, \mathbf{S}_1, \mathbf{S}_2), \quad (1.2)$$

$$h_o(\mathbf{r}, \mathbf{p}, \mathbf{P}_R, \mathbf{S}_1, \mathbf{S}_2) = \frac{\mathbf{p}^2}{2m_r} + \frac{\mathbf{P}_R^2}{2M} + V_o(\mathbf{r}, \mathbf{p}, \mathbf{P}_R, \mathbf{S}_1, \mathbf{S}_2), \quad (1.3)$$

$$V_s = V^{(0)} + \frac{V^{(1,0)}}{m_1} + \frac{V^{(0,1)}}{m_2} + \frac{V^{(2,0)}}{m_1^2} + \frac{V^{(0,2)}}{m_2^2} + \frac{V^{(1,1)}}{m_1 m_2} + \dots, \quad (1.4)$$

$$V_o = V_o^{(0)} + \frac{V_o^{(1,0)}}{m_1} + \frac{V_o^{(0,1)}}{m_2} + \frac{V_o^{(2,0)}}{m_1^2} + \frac{V_o^{(0,2)}}{m_2^2} + \frac{V_o^{(1,1)}}{m_1 m_2} + \dots, \quad (1.5)$$

where $iD_0 O \equiv i\partial_0 O - g[A_0(\mathbf{R}, t), O]$, $\mathbf{P}_R = -i\nabla_{\mathbf{R}}$ for the singlet, $\mathbf{P}_R = -i\mathbf{D}_R$ for the octet (where the covariant derivative is in the adjoint representation), $\mathbf{p} = -i\nabla_{\mathbf{r}}$,

$$m_r = \frac{m_1 m_2}{m_1 + m_2} \quad (1.6)$$

and $M = m_1 + m_2$. We adopt the color normalization

$$S = \mathbf{S}_c / \sqrt{N_c}, \quad O = O^a \mathbf{T}^a / \sqrt{T_F}, \quad (1.7)$$

for the singlet field $S(\mathbf{r}, \mathbf{R}, t)$ and the octet field $O^a(\mathbf{r}, \mathbf{R}, t)$. Here and throughout this paper we denote the quark-antiquark distance vector by \mathbf{r} , the center-of-mass position of the quark-antiquark system by \mathbf{R} , and the time by t .

Both, h_s and the potential V_s are operators acting on the Hilbert space of a heavy quark-antiquark system in the

singlet configuration.¹ According to the precision we are aiming for, the potentials have been displayed up to terms of order $1/m^2$.² The static and the $1/m$ potentials are real-valued functions of $r = |\mathbf{r}|$ only. The $1/m^2$ potentials have an imaginary part proportional to $\delta^{(3)}(\mathbf{r})$, which we will drop in this analysis, and a real part that may be decomposed as:

$$\begin{aligned} V^{(2,0)} &= V_{SD}^{(2,0)} + V_{SI}^{(2,0)}, & V^{(0,2)} &= V_{SD}^{(0,2)} + V_{SI}^{(0,2)}, \\ V^{(1,1)} &= V_{SD}^{(1,1)} + V_{SI}^{(1,1)}, \end{aligned} \quad (1.9)$$

$$V_{SI}^{(2,0)} = \frac{1}{2} \{ \mathbf{p}_1^2, V_{\mathbf{p}^2}^{(2,0)}(r) \} + V_{\mathbf{L}^2}^{(2,0)}(r) \frac{\mathbf{L}_1^2}{r^2} + V_r^{(2,0)}(r), \quad (1.10)$$

$$V_{SI}^{(0,2)} = \frac{1}{2} \{ \mathbf{p}_2^2, V_{\mathbf{p}^2}^{(0,2)}(r) \} + V_{\mathbf{L}^2}^{(0,2)}(r) \frac{\mathbf{L}_2^2}{r^2} + V_r^{(0,2)}(r), \quad (1.11)$$

$$\begin{aligned} V_{SI}^{(1,1)} &= -\frac{1}{2} \{ \mathbf{p}_1 \cdot \mathbf{p}_2, V_{\mathbf{p}^2}^{(1,1)}(r) \} \\ &\quad - V_{\mathbf{L}^2}^{(1,1)}(r) \frac{(\mathbf{L}_1 \cdot \mathbf{L}_2 + \mathbf{L}_2 \cdot \mathbf{L}_1)}{2r^2} + V_r^{(1,1)}(r), \end{aligned} \quad (1.12)$$

$$V_{SD}^{(2,0)} = V_{LS}^{(2,0)}(r) \mathbf{L}_1 \cdot \mathbf{S}_1, \quad (1.13)$$

$$V_{SD}^{(0,2)} = -V_{LS}^{(0,2)}(r) \mathbf{L}_2 \cdot \mathbf{S}_2, \quad (1.14)$$

$$\begin{aligned} V_{SD}^{(1,1)} &= V_{L_1 S_2}^{(1,1)}(r) \mathbf{L}_1 \cdot \mathbf{S}_2 - V_{L_2 S_1}^{(1,1)}(r) \mathbf{L}_2 \cdot \mathbf{S}_1 \\ &\quad + V_{S_2}^{(1,1)}(r) \mathbf{S}_1 \cdot \mathbf{S}_2 + V_{S_{12}}^{(1,1)}(r) \mathbf{S}_{12}(\mathbf{r}), \end{aligned} \quad (1.15)$$

where, $\mathbf{S}_1 = \boldsymbol{\sigma}_1/2$, $\mathbf{S}_2 = \boldsymbol{\sigma}_2/2$, $\mathbf{L}_1 \equiv \mathbf{r} \times \mathbf{p}_1$, $\mathbf{L}_2 \equiv \mathbf{r} \times \mathbf{p}_2$ and $\mathbf{S}_{12}(\mathbf{r}) \equiv \frac{3\mathbf{r} \cdot \boldsymbol{\sigma}_1 \mathbf{r} \cdot \boldsymbol{\sigma}_2}{r^2} - \boldsymbol{\sigma}_1 \cdot \boldsymbol{\sigma}_2$. Note that neither \mathbf{L}_1 nor \mathbf{L}_2 correspond to the orbital angular momentum of the particle or the antiparticle.

Due to invariance under charge conjugation plus $m_1 \leftrightarrow m_2$ interchange we have

$$V^{(1,0)}(r) = V^{(0,1)}(r). \quad (1.16)$$

This allows us to write

¹Therefore, in a more mathematical notation: $h \rightarrow \hat{h}$, $V_s(\mathbf{r}, \mathbf{p}) \rightarrow \hat{V}_s(\hat{\mathbf{r}}, \hat{\mathbf{p}})$. We will however avoid this notation in order to facilitate the reading.

²Actually, we also have to include the leading correction to the nonrelativistic dispersion relation for our calculation of the spectrum:

$$\delta V_s = -\left(\frac{1}{8m_1^3} + \frac{1}{8m_2^3} \right) \mathbf{p}^4, \quad (1.8)$$

and use the fact there is no $\mathcal{O}(\alpha_s/m^3)$ potential.

$$\frac{V^{(1,0)}}{m_1} + \frac{V^{(0,1)}}{m_2} = \frac{V^{(1,0)}}{m_r}. \quad (1.17)$$

Invariance under charge conjugation plus $m_1 \leftrightarrow m_2$ also implies

$$\begin{aligned} V_{\mathbf{p}^2}^{(2,0)}(r) &= V_{\mathbf{p}^2}^{(0,2)}(r), & V_{\mathbf{L}^2}^{(2,0)}(r) &= V_{\mathbf{L}^2}^{(0,2)}(r), \\ V_r^{(2,0)}(r) &= V_r^{(0,2)}(r; m_2 \leftrightarrow m_1), \\ V_{LS}^{(2,0)}(r) &= V_{LS}^{(0,2)}(r; m_2 \leftrightarrow m_1), \\ V_{L_1 S_2}^{(1,1)}(r) &= V_{L_2 S_1}^{(1,1)}(r; m_1 \leftrightarrow m_2). \end{aligned} \quad (1.18)$$

For the precision of the computation of the spectrum reached in this paper, we can neglect the center-of-mass momentum, i.e., we set $\mathbf{P}_R = 0$ in the following and thus $\mathbf{L}_1 \equiv \mathbf{r} \times \mathbf{p}_1 = \mathbf{r} \times \mathbf{p} \equiv \mathbf{L}$, $\mathbf{L}_2 \equiv \mathbf{r} \times \mathbf{p}_2 = -\mathbf{r} \times \mathbf{p} \equiv -\mathbf{L}$.

Expressions for the N³LO potentials for the nonequal mass case can be found in Ref. [6] for different bases of potentials (on-shell, Wilson, Coulomb, Feynman matching schemes). For illustration, we will work with the on-shell basis of potentials where the potential proportional to \mathbf{L}^2 is set to zero (for ease of reference we list them in Appendix A). Nevertheless, we emphasize that the results are independent of the chosen basis of potentials to N³LL order. In the following section, we give the N³LL potentials for the (un)equal mass case relevant for the P -wave spectrum (see also [9]). The singlet potential V_s depends on the factorization scales ν_h , ν and ν_{us} : $V_s(\nu; \nu_h, \nu_{us})$.³ Throughout this paper we will use the notation $\alpha_s = \alpha_s(\nu)$, $\alpha_{us} = \alpha_s(\nu_{us})$, $\alpha_h = \alpha_s(\nu_h)$. Large logarithms are resummed setting $\nu_h \sim m$, $\nu \sim m\alpha_s$ and $\nu_{us} \sim m\alpha_s^2$. We will generically split the RG improved potential to NⁱLL into the fixed-order result plus the correction generated by the resummation of logarithms:

$$V_{s, N^i LL}^{RG}(\nu; \nu_h, \nu_{us}) = V_{s, N^i LO}(\nu) + \delta V_{s, N^i LL}^{RG}(\nu; \nu_h, \nu_{us}), \quad (1.19)$$

such that $\delta V_{s, N^i LL}^{RG}(\nu; \nu, \nu) = 0$, and similarly for each individual potential: $V^{(1,0)}$, etc.

II. RENORMALIZATION GROUP RUNNING

We consider now the modifications of the N³LO potentials needed to achieve the resummation of the large logarithms for the P -wave spectrum.

A. Ultrasoft renormalization group running

The bare potential can be written in terms of the renormalized potential and its counterterm in the following way:

³Strictly speaking the ν dependence is traded off by a dependence in $1/r$ to the order we are working.

$$V_{s,B} = V_s + \delta V_s. \quad (2.1)$$

If the counterterm is determined in terms of the Wilson coefficients of the EFT, it is possible to resum the large logarithms of the potentials associated to the ultrasoft scale by solving the associated renormalization group equation

(RGE). The counterterm δV_s for the NLL ultrasoft running of V_s was obtained in Eq. (35) of Ref. [9].⁴ The RGE then reads

$$\nu \frac{d}{d\nu} V_{s,\overline{\text{MS}}} = B_{V_s}, \quad (2.2)$$

where

$$\begin{aligned} B_{V_s} = & C_F \left(\mathbf{r}^2 (\Delta V)^3 - \frac{1}{2m_r^2} [\mathbf{p}, [\mathbf{p}, V_o^{(0)}]] + \frac{1}{2m_r^2} \{ \mathbf{p}^2, \Delta V \} + \frac{2}{m_r} \Delta V \left(r \frac{d}{dr} V^{(0)} \right) \right. \\ & \left. + \frac{1}{2m_r} \left[4(\Delta V)^2 + 4\Delta V \left(\left(r \frac{d}{dr} \Delta V \right) + \Delta V \right) + \left(\left(r \frac{d}{dr} \Delta V \right) + \Delta V \right)^2 \right] \right) \\ & \times \left[-\frac{2\alpha_s}{3\pi} + \frac{\alpha_s^2}{9\pi^2} \left(C_A \left(-\frac{47}{3} - 2\pi^2 \right) + \frac{10}{3} T_F n_f \right) + \mathcal{O}(\alpha_s^3) \right], \end{aligned} \quad (2.3)$$

and $\Delta V = V_o^{(0)} - V^{(0)}$. Solving this RGE, we obtain the RG improved (RGI) expressions for the static, the $1/m$ and the $1/m^2$ momentum-dependent spin-independent potentials (as they do not depend on the hard scale).⁵ We obtain

$$V_{\text{RG}}^{(0)}(r; \nu_{\text{us}}) = V^{(0)}(r; \nu) + \delta V_{\text{RG}}^{(0)}(r; \nu, \nu_{\text{us}}), \quad (2.4)$$

$$V_{\text{RG}}^{(1,0)}(r; \nu_{\text{us}}) = V^{(1,0)}(r; \nu) + \delta V_{\text{RG}}^{(1,0)}(r; \nu, \nu_{\text{us}}), \quad (2.5)$$

$$V_{\mathbf{p}^2, \text{RG}}^{(2,0)}(r; \nu_{\text{us}}) = V_{\mathbf{p}^2}^{(2,0)}(r; \nu) + \delta V_{\mathbf{p}^2, \text{RG}}^{(2,0)}(r; \nu, \nu_{\text{us}}), \quad (2.6)$$

$$V_{\mathbf{p}^2, \text{RG}}^{(1,1)}(r; \nu_{\text{us}}) = V_{\mathbf{p}^2}^{(1,1)}(r; \nu) + \delta V_{\mathbf{p}^2, \text{RG}}^{(1,1)}(r; \nu, \nu_{\text{us}}), \quad (2.7)$$

where $V^{(0)}$, $V^{(1,0)}$, $V_{\mathbf{p}^2}^{(2,0)}$ and $V_{\mathbf{p}^2}^{(1,1)}$ are the fixed-order potentials. We collect them in Eqs. (A1)–(A5) for ease of reference. The symmetries in Eq. (1.18) also apply to the N³LL potentials.

The functions δV_{RG} are the corrections generated by solving Eq. (2.2). They read

$$\delta V_{\text{RG}}^{(0)}(r; \nu, \nu_{\text{us}}) = r^2 \left(\frac{C_A \alpha_s}{2r} \right)^3 \left(1 + 3 \frac{\alpha_s}{4\pi} (a_1 + 2\beta_0 \ln(\nu e^{\gamma_E} r)) \right) F(\nu; \nu_{\text{us}}), \quad (2.8)$$

$$\begin{aligned} \delta V_{\text{RG}}^{(1,0)}(r; \nu, \nu_{\text{us}}) = & \left[2 \left(\frac{C_A \alpha_s}{2r} \right)^2 \left(1 + 2 \frac{\alpha_s}{4\pi} \left(a_1 + 2\beta_0 \ln \left(\nu e^{\gamma_E + \frac{1}{2}} r \right) \right) \right) \right. \\ & \left. + 2 \frac{C_A C_F \alpha_s^2}{2r^2} \left(1 + 2 \frac{\alpha_s}{4\pi} \left(a_1 + 2\beta_0 \ln \left(\nu e^{\gamma_E - \frac{1}{2}} r \right) \right) \right) \right] F(\nu; \nu_{\text{us}}), \end{aligned} \quad (2.9)$$

$$\delta V_{\mathbf{p}^2, \text{RG}}^{(1,1)}(r; \nu, \nu_{\text{us}}) = \frac{C_A \alpha_s}{r} \left(1 + \frac{\alpha_s}{4\pi} (a_1 + 2\beta_0 \ln(\nu e^{\gamma_E} r)) \right) F(\nu; \nu_{\text{us}}), \quad (2.10)$$

$$\delta V_{\mathbf{p}^2, \text{RG}}^{(2,0)}(r; \nu, \nu_{\text{us}}) = \frac{C_A \alpha_s}{2r} \left(1 + \frac{\alpha_s}{4\pi} (a_1 + 2\beta_0 \ln(\nu e^{\gamma_E} r)) \right) F(\nu; \nu_{\text{us}}), \quad (2.11)$$

where

$$F(\nu; \nu_{\text{us}}) = C_F \frac{2\pi}{\beta_0} \left\{ \frac{2}{3\pi} \ln \frac{\alpha_{\text{us}}}{\alpha_s} - (\alpha_{\text{us}} - \alpha_s) \left(\frac{8\beta_1}{3\beta_0} \frac{1}{(4\pi)^2} - \frac{1}{27\pi^2} (C_A (47 + 6\pi^2) - 10T_F n_f) \right) \right\}. \quad (2.12)$$

Note that these expressions should be truncated at the appropriate order in the expansion in α_s for a given accuracy. $\delta V_{\text{RG}}^{(1,0)}(r; \nu, \nu_{\text{us}})$ corrects the NLL result in Ref. [9] because in B_{V_s} some subleading terms in $\alpha_s(1/r)$ of the potentials were neglected, which are needed for a NLL precision.

⁴Confirmation of the counterterm in the context of vNRQCD [32] was obtained in Refs. [33,34] for the $\mathcal{O}(1/m)$ and $\mathcal{O}(1/m^2)$, potentials. Prior to this, the running of the static potential was computed at LL in Ref. [35] and at NLL in Ref. [36] and confirmed in Ref. [37], whereas the complete LL ultrasoft running of the V_s was obtained in Ref. [38].

⁵The contributions generated by Eq. (2.2) to V_r that contribute to the P -wave spectrum will be discussed in Sec. II C.

There are other operators in the pNRQCD Lagrangian that could potentially contribute to the P -wave spectrum to N^3 LL. These are

$$\delta\mathcal{L}_a \sim \frac{c_F^{(1)}}{m_1} S^\dagger \boldsymbol{\sigma} \cdot \mathbf{B}^a O^a + \dots \quad (2.13)$$

and

$$\delta\mathcal{L}_b \sim \frac{c_S^{(1)}}{m_1^2} S^\dagger \boldsymbol{\sigma} \cdot (\mathbf{p} \times \mathbf{E}^a) O^a + \dots, \quad (2.14)$$

where the dots stand for contributions needed to make the Lagrangian density hermitian as well as the contribution of the other heavy particle. Note that both operators are spin dependent. Both operators can generate divergent contributions that are absorbed by $1/m^2$ deltalike potentials ($\sim 1/r^3$).

The contribution to the potential associated to the operator in Eq. (2.13) is generated at second-order perturbation theory with ultrasoft gluons: $\frac{\boldsymbol{\sigma} \cdot \mathbf{B}}{m} \dots \frac{\boldsymbol{\sigma} \cdot \mathbf{B}}{m}$, and it produces the following divergence:

$$\delta V_a \sim \frac{1}{m_1 m_2} \frac{1}{\epsilon} c_F^{(1)} c_F^{(2)} \alpha_{\text{us}} (\Delta V)^3 \boldsymbol{\sigma}_1 \cdot \boldsymbol{\sigma}_2. \quad (2.15)$$

The contribution to the potential associated to the operator in Eq. (2.14) is generated at second-order perturbation theory with ultrasoft gluons of the following type: $\mathbf{r} \cdot \mathbf{E} \dots \frac{c_S \mathbf{L} \cdot \mathbf{E}}{m^2}$, and produces the following divergence:

$$\delta V_b \sim \frac{1}{m_1^2} \frac{1}{\epsilon} c_S^{(1)} \alpha_{\text{us}} (\Delta V)^3 \boldsymbol{\sigma}_1 \cdot \mathbf{L}. \quad (2.16)$$

For P -wave state energies, we know that the expectation value $\langle \frac{1}{r^3} \rangle_{l \neq 0}$ is finite. This moves these contributions beyond the N^3 LL accuracy we seek in this paper. Note however, that δV_a actually contributes to the spectrum to N^3 LL but only to S -wave energies (and in particular to the hyperfine splitting [39,40]), since now $\langle \frac{1}{r^3} \rangle_{l=0}$ is divergent. δV_b does not contribute to S -wave energies either; even though $\langle \frac{1}{r^3} \rangle_{l=0}$ is divergent, the overall contribution is multiplied by \mathbf{L} , which again moves the contribution beyond N^3 LL.

Overall, we do not consider these contributions here as we are only interested in P -wave energies at N^3 LL. Therefore one only needs to consider the $\mathbf{r} \cdot \mathbf{E} \dots \mathbf{r} \cdot \mathbf{E}$ contributions up to two loops which we already discussed above.

B. Spin-dependent momentum-dependent potentials

The spin-dependent potentials do not receive ultrasoft running, unlike the spin-independent ones. If we also

restrict ourselves to the momentum-dependent potentials, they also do not receive potential running. Both statements hold true for N^3 LL precision. On the other hand the spin-dependent momentum-dependent potentials receive non-trivial hard/soft running through the inherited NRQCD Wilson coefficients coming from spin-dependent operators. All boils down to a dependence on a single NRQCD Wilson coefficient: c_F (the dependence on c_S is transformed in a dependence on c_F since $c_S = 2c_F - 1$, [41]). For the precision we seek, we need c_F with NLL precision, which is known at present [42,43]:

$$c_{F,\text{NLL}}^{(i)}(\nu, \nu_h) = z^{-\frac{\gamma_0}{2}} \left[1 + \frac{\alpha_h}{4\pi} \left(c_1 + \frac{\gamma_0}{2} \ln \frac{\nu_h^2}{m_i^2} \right) + \frac{\alpha_h - \alpha_s}{4\pi} \left(\frac{\gamma_1}{2\beta_0} - \frac{\gamma_0 \beta_1}{2\beta_0^2} \right) \right], \quad (2.17)$$

where $c_{F,\text{LL}}^{(i)}(\nu, \nu_h) = z^{-\frac{\gamma_0}{2}}$, $z = (\alpha_s/\alpha_h)^{1/\beta_0}$, $\nu_h \sim m_i$ is the hard matching scale, $c_1 = 2(C_A + C_F)$ and the one- and two-loop anomalous dimensions read

$$\gamma_0 = 2C_A, \quad \gamma_1 = \frac{68}{9} C_A^2 - \frac{52}{9} C_A T_F n_f. \quad (2.18)$$

We will also need c_F at fixed order in powers of α_s , which can be obtained from the previous expression by fixing $\nu_h = \nu$, i.e., $c_{F,\text{NLO}}^{(i)}(\nu) \equiv c_{F,\text{NLL}}^{(i)}(\nu, \nu)$. In this case, $c_{F,\text{LO}}^{(i)}(\nu) = 1$ is trivial.

The spin-dependent potentials are unambiguous under the field redefinitions considered in Ref. [6] (at least to the order we are working at). They were originally computed in Ref. [44] at NNLO, in Ref. [45] for the N^3 LO hyperfine splitting, and in Ref. [46] the complete expression for unequal masses was obtained. In principle, in order to obtain the RGI expressions of these potentials one should work in the EFT. We do not need to do that. The fact that we know the dependence of the potentials in terms of the NRQCD Wilson coefficients enables us to get them from old computations. The spin-dependent potentials have been defined in Eqs. (1.13)–(1.15). Their renormalized expressions read (renormalized NRQCD Wilson coefficients are understood)

$$V_{\text{LS,RG}}^{(2,0)}(r) = -\frac{c_F^{(1)}}{r^2} i\mathbf{r} \cdot \lim_{T \rightarrow \infty} \int_0^T dt t \langle\langle g\mathbf{B}_1(t) \times g\mathbf{E}_1(0) \rangle\rangle + \frac{c_S^{(1)}}{2r^2} \mathbf{r} \cdot (\boldsymbol{\nabla}_r V^{(0)}), \quad (2.19)$$

where

$$\begin{aligned} & \frac{i\mathbf{r}}{r^2} \cdot \lim_{T \rightarrow \infty} \int_0^T dt t \langle\langle g\mathbf{B}_1(t) \times g\mathbf{E}_1(0) \rangle\rangle|_{\overline{\text{MS}}} \\ &= \frac{C_F C_A \alpha_s^2}{2\pi r^3} (1 + \ln(r\nu e^{\gamma_E - 1})) + \mathcal{O}(\alpha_s^3), \end{aligned} \quad (2.20)$$

$$\frac{\mathbf{r}}{r^2} \cdot (\nabla_r V^{(0)}) = \frac{C_F \alpha_s}{r^3} \left[1 + \frac{\alpha_s}{4\pi} (a_1 + 2\beta_0 \ln(r\nu e^{\gamma_E - 1})) \right] + \mathcal{O}(\alpha_s^3); \quad (2.21)$$

$$V_{L_2 S_1, \text{RG}}^{(1,1)}(r) = -\frac{c_F^{(1)}}{r^2} i\mathbf{r} \cdot \lim_{T \rightarrow \infty} \int_0^T dt t \langle\langle g\mathbf{B}_1(t) \times g\mathbf{E}_2(0) \rangle\rangle, \quad (2.22)$$

where

$$\frac{i\mathbf{r}}{r^2} \cdot \lim_{T \rightarrow \infty} \int_0^T dt t \langle\langle g\mathbf{B}_1(t) \times g\mathbf{E}_2(0) \rangle\rangle_{\overline{\text{MS}}} = -C_F \frac{\alpha_s (e^{1-\gamma_E}/r)}{r^3} \left\{ 1 + \frac{\alpha_s}{\pi} \left[\left(\frac{13}{36} - \frac{1}{2} \ln \left(\frac{\nu r}{e^{1-\gamma_E}} \right) \right) C_A - \frac{5}{9} n_f T_F \right] \right\}, \quad (2.23)$$

and

$$V_{S_{12}, \text{RG}}^{(1,1)}(r) = \frac{c_F^{(1)} c_F^{(2)}}{4} i\hat{\mathbf{r}}^i \hat{\mathbf{r}}^j \lim_{T \rightarrow \infty} \int_0^T dt \left[\langle\langle g\mathbf{B}_1^i(t) g\mathbf{B}_2^j(0) \rangle\rangle - \frac{\delta^{ij}}{3} \langle\langle g\mathbf{B}_1(t) \cdot g\mathbf{B}_2(0) \rangle\rangle \right], \quad (2.24)$$

where

$$i\hat{\mathbf{r}}^i \hat{\mathbf{r}}^j \lim_{T \rightarrow \infty} \int_0^T dt \left[\langle\langle g\mathbf{B}_1^i(t) g\mathbf{B}_2^j(0) \rangle\rangle - \frac{\delta^{ij}}{3} \langle\langle g\mathbf{B}_1(t) \cdot g\mathbf{B}_2(0) \rangle\rangle \right]_{\overline{\text{MS}}} \quad (2.25)$$

$$= \frac{C_F \alpha_s (e^{4/3-\gamma_E}/r)}{r^3} \left\{ 1 + \frac{\alpha_s}{\pi} \left[\left(\frac{13}{36} - \ln \left(\frac{\nu r}{e^{4/3-\gamma_E}} \right) \right) C_A - \frac{5}{9} n_f T_F \right] \right\}. \quad (2.26)$$

The other potentials follow from the symmetry relations in Eq. (1.18).

Note that the above potentials have N³LL accuracy. This is a new result. Additionally, we give expressions with N³LO accuracy, $\mathcal{O}(\alpha_s^2)$, for the Wilson loops with chromomagnetic (and/or chromoelectric) insertions in the $\overline{\text{MS}}$. One can easily change to other schemes by changing e.g., $c_F^{(i)}$ from the $\overline{\text{MS}}$ to the lattice scheme (since the whole potential is scheme independent). This enables a more detailed comparison with lattice simulations at short distances. This research will be carried out elsewhere.

Overall, with very few new computations we have been able to obtain the spin-dependent momentum-dependent $1/m^2$ potentials with N³LL accuracy. The NNLL result was originally obtained in Ref. [47].

C. V_r and $V_{S^2}^{(1,1)}$ potentials

The remaining potentials we need to consider are V_r and $V_{S^2}^{(1,1)}$. At $\mathcal{O}(\alpha_s)$ they are proportional to $\delta(\mathbf{r})$, which does not contribute to the spectrum of $l \neq 0$ states to the order we work (the delta-like potential contribution vanishes at first and second order in perturbation theory). At $\mathcal{O}(\alpha_s^2)$, potentials proportional to $\ln k$ (or $\text{reg } 1/r^3$ in position space) are generated in the NRQCD-pNRQCD matching. Such potentials generate nonzero contributions to the spectrum of $l \neq 0$ states. We know them at leading nonvanishing order, which is all we need. We need them

both for the spin-dependent and the spin-independent potentials.

The spin-dependent potential has been computed with N³LL accuracy in Ref. [39,40]. We are only interested in the term proportional to $\text{reg } \frac{1}{r^3}$, which reads

$$V_{S^2, \text{RG}}^{(1,1)}(r) \doteq \frac{8\pi C_F}{3} \left[-\frac{1}{4\pi} \text{reg } \frac{1}{r^3} \right] c_F^{(1)} c_F^{(2)} \frac{\alpha_s^2}{\pi} \left(-\frac{\beta_0}{2} + \frac{7}{4} C_A \right), \quad (2.27)$$

where

$$-\frac{1}{4\pi} \text{reg } \frac{1}{r^3} \equiv \int \frac{d^3 k}{(2\pi)^3} e^{-i\mathbf{k} \cdot \mathbf{r}} \ln k. \quad (2.28)$$

The correction to the fixed-order potential comes from considering the difference between $c_F^{(1)} c_F^{(2)}$ evaluated at ν_h and at $\nu_h = \nu$.

The spin-independent V_r is at present unknown with N³LL accuracy (indeed, it is the missing link to obtain the complete N³LL spectrum for a general S -wave energy), since the $\mathcal{O}(\alpha_s^2)$ of the delta potential is not known. This does not affect our analysis, since the term proportional to $\delta^{(3)}(\mathbf{r})$ does not contribute to the energy of P -wave states. On the other hand, we know the term proportional to $\text{reg } \frac{1}{r^3}$ with enough accuracy, as it can be deduced from the k dependence of the NNLL result. It reads

$$\frac{V_{r,\text{RG}}^{(2,0)}(r)}{m_1^2} + \frac{V_{r,\text{RG}}^{(0,2)}(r)}{m_2^2} + \frac{V_{r,\text{RG}}^{(1,1)}(r)}{m_1 m_2} = \frac{\pi C_F}{m_1 m_2} \left[-\frac{1}{4\pi} \text{reg} \frac{1}{r^3} \right] \left(k \frac{d}{dk} \tilde{D}_d^{(2)} \right) \Big|_{k=\nu}^{LL}, \quad (2.29)$$

where

$$\begin{aligned} k \frac{d}{dk} \tilde{D}_d^{(2)} \Big|_{k=\nu}^{LL} &= -\beta_0 \frac{\alpha_s^2}{2\pi} + \frac{\alpha_s^2}{\pi} \left(2C_F - \frac{C_A}{2} \right) c_k^{(1)} c_k^{(2)} + \frac{\alpha_s^2}{\pi} \left[\frac{m_1}{m_2} \left(\frac{1}{3} T_f n_f \bar{c}_1^{hl(2)} - \frac{4}{3} (C_A + C_F) [c_k^{(2)}]^2 - \frac{5}{12} C_A [c_F^{(2)}]^2 \right) \right. \\ &\quad \left. + \frac{m_2}{m_1} \left(\frac{1}{3} T_f n_f \bar{c}_1^{hl(1)} - \frac{4}{3} (C_A + C_F) [c_k^{(1)}]^2 - \frac{5}{12} C_A [c_F^{(1)}]^2 \right) \right] \\ &\quad - \frac{(m_1 + m_2)^2}{m_1 m_2} \frac{4}{3} \left(\frac{C_A}{2} - C_F \right) \frac{\alpha_s^2}{\pi} \left[\ln \left(\frac{\alpha_s}{\alpha_{\text{us}}} \right) + 1 \right], \end{aligned} \quad (2.30)$$

($c_k^{(i)} = 1$ because of reparametrization invariance [48]) and the gauge independent combination of NRQCD Wilson coefficients

$$\begin{aligned} \bar{c}_1^{hl(i)}(\nu) &\equiv c_1^{hl(i)}(\nu) + c_D^{(i)}(\nu) \\ &= z^{-2C_A} + \left(\frac{20}{13} + \frac{32 C_F}{13 C_A} \right) [1 - z^{-\frac{13C_A}{6}}] \end{aligned} \quad (2.31)$$

was computed in Refs. [49,50].

Finally, note that the ultrasoft contribution to V_r in Eq. (2.30) is $1/N_c^2$ suppressed and that Eq. (2.30) is the expression in the on-shell scheme.

III. TOTAL SHIFT ON THE ENERGY LEVELS

The P -wave spectrum at $N^3\text{LO}$ was obtained in Refs. [4,5] for the equal mass case and in Ref. [6] for the unequal mass case. The resulting expression for $E_{N^3\text{LO}}$ can be found in Appendix B. From the RGI potentials discussed in Sec. II we obtain the $N^i\text{LL}$ shift in the energy levels

$$E_{N^i\text{LL}}(\nu, \nu_h, \nu_{\text{us}}) = E_{N^i\text{LO}} + \delta E_{\text{RG}}(\nu, \nu_h, \nu_{\text{us}}) \Big|_{N^i\text{LL}}. \quad (3.1)$$

where $E_{N^i\text{LO}} = E_{N^i\text{LL}}(\nu, \nu, \nu)$. The explicit expressions of the fixed-order and resummed energies can be found in Appendices B and C.

The LO and NLO energy levels are unaffected by the RG improvement, i.e.,

$$\delta E_{\text{RG}} \Big|_{\text{LL}} = \delta E_{\text{RG}} \Big|_{\text{NLL}} = 0. \quad (3.2)$$

We now determine the variations with respect to the NNLO and $N^3\text{LO}$ results. We are here interested in the corrections associated to the resummation of logarithms. In order to obtain the spectrum of a P wave at NNLL and $N^3\text{LL}$, we need to add the following energy shift to the NNLO and $N^3\text{LO}$ spectrum (strictly speaking we

only compute the piece that contributes to the P -wave spectrum):

$$\delta E_{\text{RG}} \Big|_{\text{NNLL}} = \langle nl | \delta V_{s,\text{NNLL}}^{\text{RG}} | nl \rangle = E_n^C \left(\frac{\alpha_s}{\pi} \right)^2 \delta c_2, \quad (3.3)$$

which was computed in Ref. [38] for equal masses, and

$$\begin{aligned} \delta E_{\text{RG}} \Big|_{N^3\text{LL}} &= \langle nl | \delta V_{s,N^3\text{LL}}^{\text{RG}} | nl \rangle \\ &\quad + 2 \langle nl | [V_1^{(0)} - V_0^{(0)}] \frac{1}{(E_n^C - h')} \delta V_{s,\text{NNLL}}^{\text{RG}} | nl \rangle \\ &\quad + [\delta E_{\text{us}}(\nu, \nu_{\text{us}}) - \delta E_{\text{us}}(\nu, \nu)] \end{aligned} \quad (3.4)$$

$$= E_n^C \left[\left(\frac{\alpha_s}{\pi} \right)^2 \delta c_2 + \left(\frac{\alpha_s}{\pi} \right)^3 (2\beta_0 \delta c_2 L_\nu + \delta c_3) \right]. \quad (3.5)$$

Note that $\langle nl | \delta V_{s,N^3\text{LL}}^{\text{RG}} | nl \rangle$ includes $\langle nl | \delta V_{s,\text{NNLL}}^{\text{RG}} | nl \rangle$. Let us also note that the first term in Eq. (3.4), besides the $N^3\text{LO}$ ultrasoft corrections to the momentum-dependent potentials, also contains the $\ln k$ contributions associated to V_r and V_{g^2} discussed in Sec. II C. In the second term of Eq. (3.4), we only have to consider the LL ultrasoft running of the momentum-dependent potentials and the LL (hard) running of the spin-dependent potentials. The first and second terms in Eq. (3.4) are computed in the same way we did in Ref. [6]. We add the last term in Eq. (3.4) in order to account for the evaluation at the ultrasoft scale of the ultrasoft energy:

$$\begin{aligned} \delta E_{nl}^{\text{us}}(\nu, \nu_{\text{us}}) = & -E_n^C \frac{\alpha_s \alpha_{\text{us}}}{\pi} \left[\frac{2}{3} C_F^3 L_{nl}^E + \frac{1}{3} C_A \left(L_{\nu_{\text{us}}} - L_{\text{us}} + \frac{5}{6} \right) \right. \\ & \times \left(\frac{C_A^2}{2} + \frac{4C_A C_F}{(2l+1)n} + 2C_F^2 \left(\frac{8}{(2l+1)n} - \frac{1}{n^2} \right) \right) \\ & \left. + \frac{8\delta_{l0}}{3n} C_F^2 \left(C_F - \frac{C_A}{2} \right) \left(L_{\nu_{\text{us}}} - L_{\text{us}} + \frac{5}{6} \right) \right], \end{aligned} \quad (3.6)$$

where $L_{\text{us}} = \ln \frac{C_F \alpha_s n}{2} + S_1(n+l)$, and L_{nl}^E are the non-Abelian Bethe logarithms. Numerical determinations of these non-Abelian Bethe logarithms for $l \neq 0$ can be found in Ref. [5].

In Eq. (3.5), $E_n^C = -\frac{m_r C_F^2 \alpha_s^2}{2n^2}$, $L_\nu = \ln \frac{n\nu}{2C_F m_r \alpha_s} + S_1(n+l)$. We split the δc_i coefficients into a Coulomb-like and a non-Coulomb-like contribution,

$$\delta c_i = \delta c_i^c + \delta c_i^{\text{nc}}, \quad (3.7)$$

for $i = 2, 3$. The corrections δc_i^c are given in Eqs. (C7) and (C8). They are generated by the ultrasoft corrections to the static potential. The relativistic ultrasoft contribution to $\delta c_{2/3}^{\text{nc}}$ is produced by Eqs. (2.9)–(2.11), plus the ultrasoft part of Eq. (2.30) and Eq. (3.6), to the appropriate order. Explicit

expressions for these quantities can be found in Eqs. (C13) and (C14). The hard contribution to $\delta c_{2/3}^{\text{nc}}$ is generated by the (nontrivial) hard/soft running of the relativistic potentials encoded in the NRQCD Wilson coefficients. The explicit expressions can be found in Eq. (C15) and Eq. (C19). The former only receives contributions from the spin-dependent potentials, whereas the latter receives contributions from both the spin-dependent and the spin-independent potentials. The spin-dependent and spin-independent contributions from the running of the Wilson coefficients can be found in Eq. (C21) and Eq. (C22), respectively.

Note that, throughout this paper, we have introduced a change of the basis of spin operators with respect to the basis used in Ref. [6] to compute the spectrum for different masses: $\{\mathbf{S}, \mathbf{S}_1\} \rightarrow \{\mathbf{S}, \mathbf{S}^-\}$ where the symmetric and antisymmetric spin operators are $\mathbf{S} = \mathbf{S}_1 + \mathbf{S}_2$ and $\mathbf{S}^- = \mathbf{S}_1 - \mathbf{S}_2$. We find that the latter basis suits better the description of the heavy quarkonium spectrum since $\langle \mathbf{S}^- \rangle = 0$. We give the expressions of the N³LO energy in the new spin basis in Appendix B.

From the N³LL computation we can obtain the large logs of $\mathcal{O}(\alpha_s^6)$ for the expansion of the mass in powers of α_s at the scale $\nu = m C_F \alpha_s$. For the $n = 2, l = 1$ state and equal masses, it reads (with $n_f = 3$)

$$\begin{aligned} \delta E_{21} = & E_2^C \left(\frac{\alpha_s}{\pi} \right)^4 \left[\ln \frac{1}{C_F \alpha_s} (81.4171 D_s - 2.19325 S_{12} + 160.084 X_{LS} - 7160.10) \right. \\ & \left. + \ln^2 \frac{1}{C_F \alpha_s} (-8.22467 D_s - 13.1595 X_{LS} - 244.684) \right]. \end{aligned} \quad (3.8)$$

IV. FINE AND HYPERFINE SPLITTING

The results of the previous section apply to a general state with $l \neq 0$. Now we would like to study in more detail the fine and hyperfine splittings of P -wave states. Note that these splittings do not depend on the ultrasoft scale at the order at which we are working. In principle, this means that we do not have to rely on the assumption that the ultrasoft scale can still be handled in the weak-coupling approximation (otherwise the power counting of the nonperturbative corrections changes). If one assumes that $m\nu^2 \gg \Lambda_{\text{QCD}}$, the complete expression for the leading nonperturbative expression was computed in [51]⁶ (earlier

⁶We profit to correct Eq. (3.6) of that reference that should read

$$\Delta_{\text{HF}}(\text{new}) = -\frac{\pi \langle \alpha_s G^2 \rangle}{m^3 (C_F \tilde{\alpha}_s)^2 \tilde{\alpha}_s} \frac{\alpha_s}{1437897825} \frac{79139056}{1437897825}.$$

The change is produced by an algebraic mistake in $V_8^{\text{HF}}(\text{annihilation})$ (the “−3” should be zero). This makes the $1/N_c^2$ correction vanish in Eqs. (1.7) and (3.1), changes 29 → 32 in Eq. (3.2) and Eq. (3.6) to the expression above.

partial results can be found in [52]). In any case, we will not try to incorporate nonperturbative effects in this paper, lacking a more clear understanding of the behavior of the perturbative series.

A. Fine splitting

In general, we find for $s = 1$ and $l \neq 0$ (following standard heavy quarkonium spectroscopy we define $n_r = n - 1$ for P -wave states):

$$\begin{aligned} & E(n_r^3 L_j) - E(n_r^3 L_{j'}) \\ & = E_n^C \left(\frac{\alpha_s}{\pi} \right)^2 \left[\delta c_2^{\text{SD,h}} \Big|_j - \delta c_2^{\text{SD,h}} \Big|_{j'} \right] \\ & + E_n^C \left(\frac{\alpha_s}{\pi} \right)^3 \left[\left(\delta c_3^{\text{SD,h}} + 2\beta_0 \delta c_2^{\text{SD,h}} L_\nu + \mathcal{E}_h \left(\frac{\alpha_h}{\alpha_s} L_{\nu_h} - L_\nu \right) \right) \Big|_j \right. \\ & \left. - \left(\delta c_3^{\text{SD,h}} + 2\beta_0 \delta c_2^{\text{SD,h}} L_\nu + \mathcal{E}_h \left(\frac{\alpha_h}{\alpha_s} L_{\nu_h} - L_\nu \right) \right) \Big|_{j'} \right], \end{aligned} \quad (4.1)$$

where j is the quantum number associated to the combination of operators $\mathbf{J} = \mathbf{L} + \mathbf{S}$.

For different masses and $n = 2$ we find:

$$\begin{aligned}
E(1^3P_j) - E(1^3P_{j'}) &= \frac{\alpha_s^4 C_F^4 m_r^3}{192 m_1 m_2} \left\{ 4(D_s|_j - D_s|_{j'}) z^{-\gamma_0} \left[1 + \frac{\alpha_s}{2\pi} \left(2 \left(\frac{209}{36} - \frac{\pi^2}{3} \right) \beta_0 + \frac{\alpha_h - \alpha_s}{\alpha_s} \left(\frac{\gamma_1}{2\beta_0} - \frac{\beta_1 C_A}{\beta_0^2} + C_A \ln \left(\frac{\nu_h^2}{m_1 m_2} \right) \right) \right. \right. \right. \\
&\quad \left. \left. \left. + 2C_A + 2C_F \right) + 2(2\beta_0 - C_A) \ln \frac{\nu}{m_r C_F \alpha_s} - C_A \ln \frac{m_1 m_2}{\nu_h^2} - \frac{11C_A}{3} + 2C_F \right] \right. \\
&\quad \left. - (j(j+1) - j'(j'+1)) \frac{m_1^2 + m_2^2}{m_1 m_2} \left[1 + \frac{\alpha_s}{2\pi} \left(\beta_0 \left(4 \ln \frac{\nu}{m_r C_F \alpha_s} - \frac{2\pi^2}{3} + \frac{215}{18} \right) - \frac{16C_A}{3} \right) \right] \right. \\
&\quad \left. + (j(j+1) - j'(j'+1)) \frac{2m_1 m_2}{m_r^2} z^{-\frac{\gamma_0}{2}} \left[1 + \frac{\alpha_s}{4\pi} \left(2\beta_0 \left(4 \ln \frac{\nu}{\alpha_s C_F m_r} - \frac{2\pi^2}{3} + \frac{215}{18} \right) + 2C_F \right. \right. \right. \\
&\quad \left. \left. \left. - 2C_A \left(\ln \frac{\nu}{m_r C_F \alpha_s} + \frac{m_r}{m_1 m_2} \left(m_2 \ln \frac{m_1}{\nu_h} + m_1 \ln \frac{m_2}{\nu_h} \right) + \frac{16}{3} \right) \right) \right] \right. \\
&\quad \left. \left. \left. + \frac{\alpha_h - \alpha_s}{\alpha_s} \left(\frac{\gamma_1}{2\beta_0} - \frac{\beta_1 C_A}{\beta_0^2} - \frac{2m_r}{m_1 m_2} C_A \left(m_2 \ln \frac{m_1}{\nu_h} + m_1 \ln \frac{m_2}{\nu_h} \right) + 2C_A + 2C_F \right) \right] \right\}, \quad (4.2)
\end{aligned}$$

where $D_s = 1/2 \langle S_{12}(\mathbf{r}) \rangle$. Note that the equal mass case is obtained just by taking $m_1 = m_2 = m$.

We have checked that in the limit $\nu_h = \nu$ we recover the result at N³LO obtained in Eq. (26) of Ref. [7].

Finally we can obtain the leading large logarithms for the fixed-order contribution by expanding α_h in terms of α_s . The leading logarithmic resummation contains all terms of order $\alpha_s^{4+n} \ln^n \alpha_s$, while the NLO resummation contains all terms of order $\alpha_s^5 \ln^n \alpha_s$. Setting $\nu_h = \sqrt{m_1 m_2}$ and $\nu = 2C_F m_r \alpha_s$ we obtain the higher-order logarithms:

$$\begin{aligned}
E(1^3P_j) - E(1^3P_{j'})|_{>\mathcal{O}(\alpha_s^5) \times \log s} &= E_2^C \left(\frac{\alpha_s}{\pi} \right)^4 \ln \left(\frac{1}{C_F \alpha_s} \right) \frac{\pi^2 C_F^2}{96} \left\{ \frac{8m_r^2}{m_1 m_2} (D_s|_j - D_s|_{j'}) \left[-\frac{23C_A^2}{4} - \frac{2}{3} \pi^2 \beta_0 C_A + \frac{493\beta_0 C_A}{36} \right. \right. \\
&\quad \left. \left. - 2C_A(C_A - 2\beta_0) \ln 2 + 2C_A C_F + \beta_0 C_F - \frac{C_A}{2} (\beta_0 + 2C_A) \ln \frac{m_1 m_2}{4m_r^2} \right] \right. \\
&\quad \left. + (j(j+1) - j'(j'+1)) \left[-\frac{89C_A^2}{6} - \frac{4}{3} \pi^2 \beta_0 C_A + \frac{505\beta_0 C_A}{18} + 2C_A(4\beta_0 - C_A) \ln 2 \right. \right. \\
&\quad \left. \left. + 2C_A C_F + 2\beta_0 C_F + C_A(\beta_0 + C_A) \left(\frac{m_1 - m_2}{m_1 + m_2} \ln \frac{m_1}{m_2} - \ln \frac{m_1 m_2}{4m_r^2} \right) \right] \right\} \\
&\quad - E_2^C \left(\frac{\alpha_s}{\pi} \right)^4 \ln^2 \left(\frac{1}{C_F \alpha_s} \right) \frac{\pi^2 C_A C_F^2}{96} \left\{ (j(j+1) - j'(j'+1)) (\beta_0 + C_A) \right. \\
&\quad \left. + \frac{4m_r^2}{m_1 m_2} (\beta_0 + 2C_A) (D_s|_j - D_s|_{j'}) \right\}. \quad (4.3)
\end{aligned}$$

B. Hyperfine splitting

The hyperfine splitting of P -wave states is defined in the following way:

$$\Delta_{n,l} \equiv E(n^1 l_{j=l}) - E(n^3 l)_{c.o.g.}, \quad (4.4)$$

where the ‘‘center of gravity’’ average reads

$$\begin{aligned}
E(n^3 l)_{c.o.g.} &= \frac{2l-1}{3(2l+1)} E(n^3 l_{j=l-1}) + \frac{2l+1}{3(2l+1)} E(n^3 l_{j=l}) \\
&\quad + \frac{2l+3}{3(2l+1)} E(n^3 l_{j=l+1}). \quad (4.5)
\end{aligned}$$

In practice, we will use this expression only for the case $n = 2$ and $l = 1$:

$$\Delta \equiv \Delta_{2,1} = E(1^1 P_1) - \frac{1}{9} (5E(1^3 P_2) + 3E(1^3 P_1) + E(1^3 P_0)). \quad (4.6)$$

For general radial and $l \neq 0$ angular quantum numbers, and different masses, we find at fixed order

$$\Delta_{n,l} = -\frac{m_r^3 C_F^4 \alpha_s^5 (1 - \delta_{l0})}{9 m_1 m_2 \pi l (l+1) (2l+1) n^3} (C_A - 8n_f T_F). \quad (4.7)$$

We have checked that Eq. (4.7) for $m_1 = m_2 = m$ recovers the result obtained in Ref. [8]. Note that the hyperfine

TABLE I. Experimental values of the heavy quarkonium masses, Δ and the fine splittings in MeV.

System	$b\bar{b}(1P)$ (exp)	$c\bar{b}(1P)$ (exp)	$c\bar{c}(1P)$ (exp)
$h(1P_1)$	9899.3(8)	...	3525.38(11)
$\chi_0(3P_0)$	9859.44(42)(31)	...	3414.71(30)
$\chi_1(3P_1)$	9892.78(26)(31)	...	3510.67(5)
$\chi_2(3P_2)$	9912.21(26)(31)	...	3556.17(7)
Δ	-0.57(84)	...	+0.08(13)
$\chi_1(3P_1) - \chi_0(3P_0)$	32.49(93)	...	95.96 (30)
$\chi_2(3P_2) - \chi_1(3P_1)$	19.10(25)	...	45.5 (1)

splitting for P -wave states is $\mathcal{O}(\alpha_s)$ suppressed compared with the hyperfine splitting of S -wave states. This suppression is indeed seen experimentally (actually, experimentally, the suppression is stronger than expected. For a discussion on this issue, see [53]).

The resummation of logarithms can be easily obtained by incorporating the nontrivial running of the NRQCD Wilson coefficients. The general N³LL result for a P -wave state reads

$$\Delta_{n,l}^{\text{RG}} = -\frac{m_r^3 C_F^4 \alpha_s^5 (1 - \delta_{l0})}{9m_1 m_2 \pi l(l+1)(2l+1)n^3} (C_A - 8n_f T_F) z^{-\gamma_0}. \quad (4.8)$$

Note that this quantity is positive, because it is one of the few places where light-fermion effects are more important than non-Abelian effects.

Since we only have the first order in the logarithmic expansion, we can only compute terms that are $\alpha_s^{5+n} \ln^n \alpha_s$. Setting $\nu_h = \sqrt{m_1 m_2}$ and $\nu = 2m_r C_F \alpha_s$, we obtain for a P wave

$$\Delta_{n,l} |_{\ln \alpha_s} = \frac{m_r^3 C_F^4 \alpha_s^6 C_A (C_A - 8T_F n_f)}{9\pi^2 m_1 m_2 n^3} \frac{(1 - \delta_{l0})}{l(l+1)(2l+1)} \ln \frac{1}{C_F \alpha_s} \times \left\{ 1 - \frac{\alpha_s}{4\pi} (2C_A + 3\beta_0) \ln \frac{1}{C_F \alpha_s} \right\}. \quad (4.9)$$

V. PHENOMENOLOGY OF $n=2, l=1$ STATES AT STRICT WEAK COUPLING

We now confront our results with the experimental values of the spectrum [54] for $n=2, l=1$ states, which we list in Table I. We use the modified renormalon

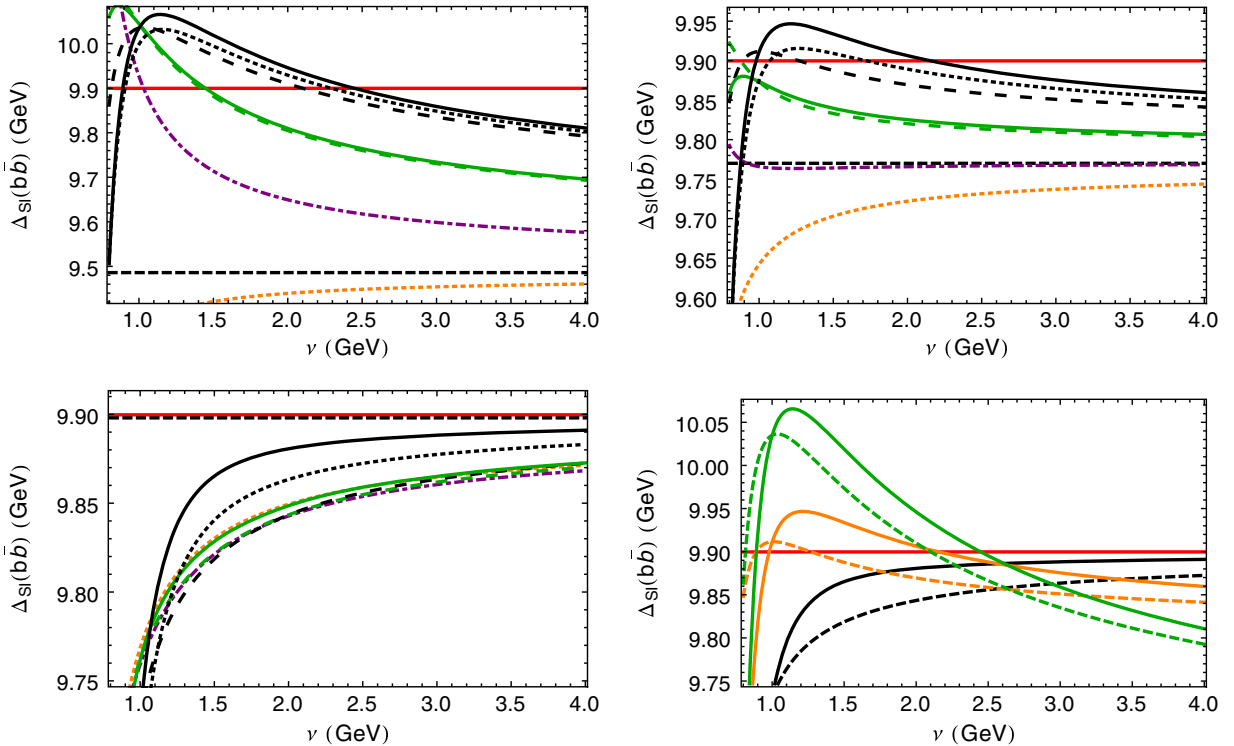


FIG. 1. Plots for Δ_{Sl} in the RS' scheme with $\nu_{\text{us}} = 1$ GeV for bottomonium. *Upper left, upper right and lower left panels:* Plots for $\nu_f = 2, 1$ and 0.7 GeV respectively. The red line is the experimental value, the black-dashed line is $2m_{b,RS'}$. The orange-dotted, purple dot-dashed, green-dashed and black-dashed lines are Δ_{Sl} evaluated at LO-N³LO, respectively. The solid-green and solid-black lines are the NNLL and N³LL result respectively, and the dotted-black line is the N³LL result without $\delta E_{21}^{\text{us}}$. *Lower right panel:* Comparison of the $\nu_f = 2$ GeV (green), $\nu_f = 1$ GeV (orange) and $\nu_f = 0.7$ GeV (black) lines. For each case, the dashed line is the N³LO result and the solid line the N³LL one.

subtracted scheme (RS'), as defined in Ref. [18] for the heavy quark masses and the static potential. The RS' scheme eliminates the leading renormalon of the pole mass and the static potential, introducing a new factorization scale, ν_f , which is formally smaller than, or of the order of, the soft energy regime. We refer to Ref. [18] for extra details. The values for the bottom and charm quark masses used in this paper are those determined in Ref. [29]. For the strong coupling we take $\alpha_s(M_z) = 0.1184(12)$ from Ref. [54].

A. Spin-independent energy combination

We first consider the following energy combination, which is free of spin-dependent effects:

$$\Delta_{SI} \equiv \frac{1}{12}(5M_{\chi_{b2}} + 3M_{\chi_{b1}} + M_{\chi_{b0}}) + \frac{1}{4}M_{h_b}, \quad (5.1)$$

and similarly for charmonium and B_c .

This quantity allows us to visualize the gross features of the spectrum of any P -wave state. We consider first bottomonium. In Fig. 1, we compare the strict weak-coupling prediction with experiment. We show both the

fixed-order and RGI expressions. The former can be found in Eq. (B1) and the latter in Eq. (C1). We have explored the dependence of the result with ν_f , ν and the order of truncation of the computation. We produce plots with $\nu_f = 2$ GeV, $\nu_f = 1$ GeV and $\nu_f = 0.7$ GeV. For reference, we take the $\nu_f = 1$ GeV case. In this case, the fixed-order result approaches the experimental number as we increase the order of truncation of the computation (albeit the size of the consecutive terms is almost equal, i.e., the convergence is marginal). Indeed, the N³LO result agrees with experiment at $\nu \sim 1.2$ GeV and shows a relatively mild scale dependence. The resummation of logarithms produces nontrivial results at NNLL and N³LL. We observe that most of the effect of the RGI is due to the ultrasoft gluons. At NNLL the effect of resummation of logarithms is marginal. At N³LL the effect is important. At this order, there is relatively good agreement with experiment. At $\nu \sim 2.2$ GeV there is agreement with experiment and the scale variation is of order $\sim \pm 50$ MeV in the range $\nu = 1-4$ GeV. In this respect, the resummation of logarithms (in particular ultrasoft logarithms) does not spoil the agreement with data, though it makes the shift between the

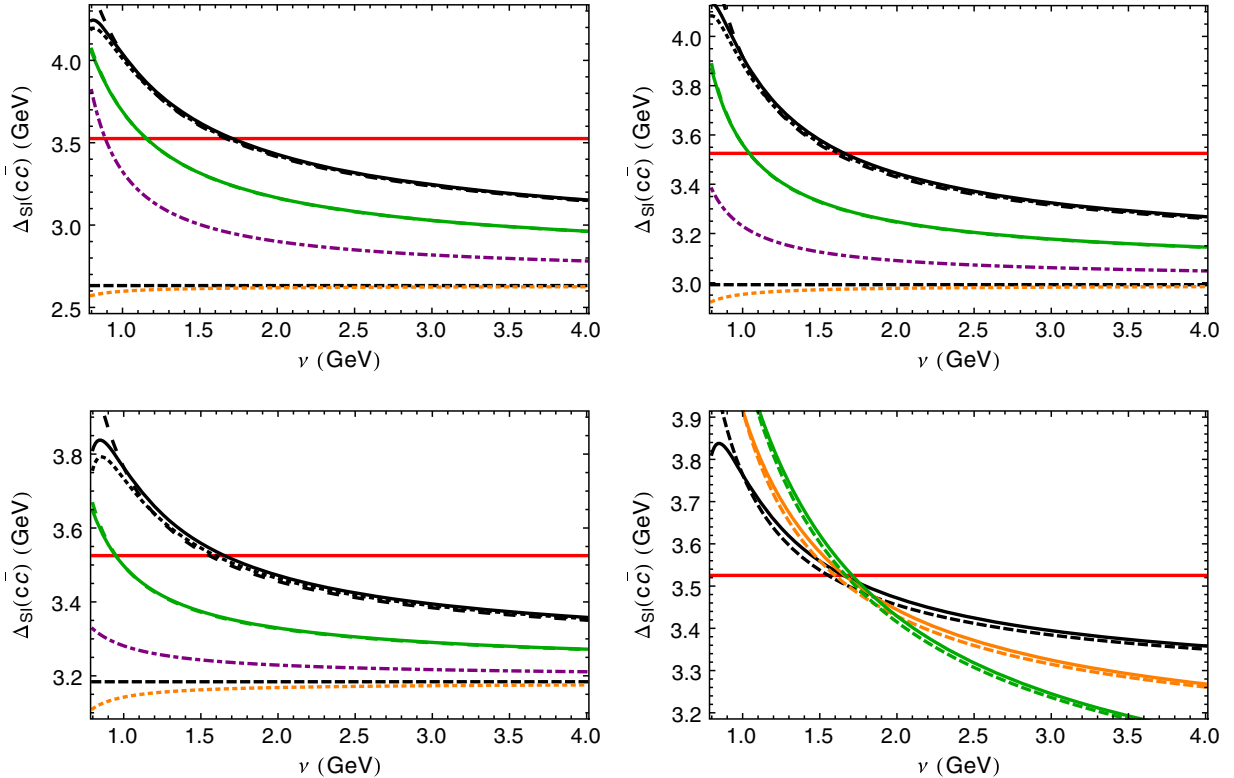


FIG. 2. Plots for Δ_{SI} in the RS' scheme with $\nu_{us} = 1$ GeV for charmonium. *Upper left, upper right and lower left panels:* Plots for $\nu_f = 2, 1$ and 0.7 GeV respectively. The red line is the experimental value, the black-dashed line is $2m_{b,RS'}$. The orange-dotted, purple dot-dashed, green-dashed and black-dashed lines are Δ_{SI} evaluated at LO-N³LO, respectively. The solid-green and solid-black lines are the NNLL and N³LL result respectively, and the dotted-black line is the N³LL result without δE_{21}^{us} . *Lower right panel:* Comparison of the $\nu_f = 2$ GeV (green), $\nu_f = 1$ GeV (orange) and $\nu_f = 0.7$ GeV (black) lines. For each case, the dashed line is the N³LO result and the solid line the N³LL one.

NNLL and N³LL bigger putting into question the convergence of the perturbative expansion. Finally, the biggest point of concern is the applicability of the weak-coupling computation at the ultrasoft scale. We roughly assess the importance of this effect by subtracting δE_{us} to the N³LL result. The effect is small (this happens both for the RGI and the fixed-order computation). Overall, the uncertainties of the computation do not allow us to see if the resummation of the large logarithms improves the result or not. We have also explored the dependence of the result on ν_f . Choosing a larger value, $\nu_f = 2$ GeV, does not change the qualitative picture. It makes it slightly more convergent but at the prize of making the corrections and scale dependence bigger (note though that $\nu_f = 2$ GeV is an unnatural value for ν_f , as the power counting demands $\nu_f < \text{soft scale}$, which we do not expect to happen for $\nu_f = 2$ GeV). Remarkably, for the smaller value $\nu_f = 0.7$ GeV, the size of the higher-order corrections is very small, except for the N³LL result, where the incorporation of the large (ultrasoft) logarithms and of the ultrasoft correction brings the result quite close to experiment. In the last plot in Fig. 1, we combine the N³LL and N³LO results for different values of ν_f . We observe that smaller values of ν_f produce smaller ν

scale dependence (we remark again the warning of choosing a too high value of ν_f). They are all consistent among them and with experiment. Indeed, the three N³LL lines cross at

$$\Delta_{SI} \sim 9.885 \text{ GeV}, \quad (5.2)$$

quite close the experimental value $\Delta_{SI} \sim 9.900 \text{ GeV} \sim M_{h_b}$. The three N³LO lines cross at $\Delta_{SI} \sim 9.850 \text{ GeV}$, also quite close the experimental value. As a final remark, in all cases, at $\nu \lesssim 1$ GeV, there is a strong scale dependence.

For completeness, we also show the results for charmonium and B_c in Figs. 2 and 3 (and for the renormalon-free combination $\Delta_{SI}^{(B_c)} - \Delta_{SI}^{(bb)}/2 - \Delta_{SI}^{(cc)}/2$ in Fig. 4) but in those cases the errors are so large that we do not aim to any serious phenomenological analysis. At most we can give an estimate of

$$\Delta_{SI}^{(B_c)} \sim 6.75 \text{ GeV}. \quad (5.3)$$

This number is obtained from the approximate crossing of the three different curves in the lower-right panel in Fig. 3. For the case of bottomonium and charmonium

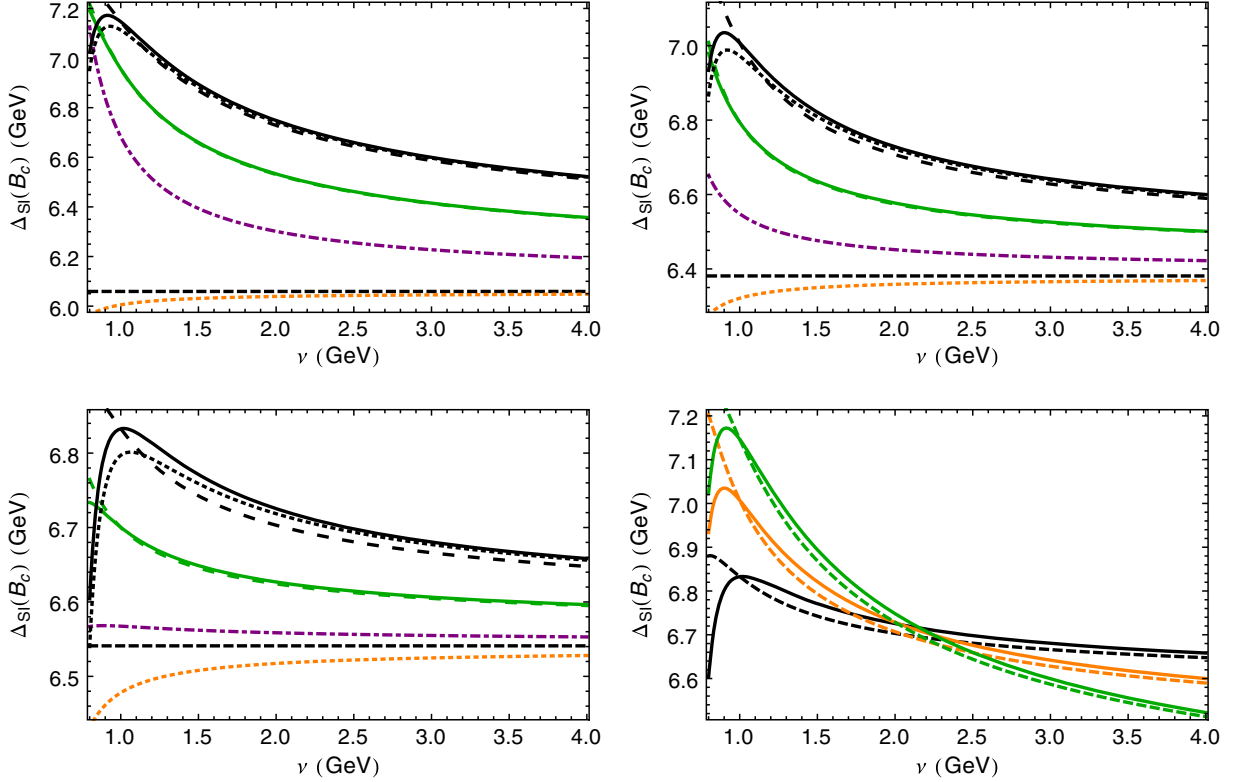


FIG. 3. Plots for Δ_{SI} in the RS' scheme with $\nu_{us} = 1$ GeV for B_c . *Upper left, upper right and lower left panels:* Plots for $\nu_f = 2, 1$ and 0.7 GeV respectively. The black-dashed line is $m_{b,RS'} + m_{c,RS'}$. The orange-dotted, purple dot-dashed, green-dashed and black-dashed lines are Δ_{SI} evaluated at LO-N³LO, respectively. The solid-green and solid-black lines are the NNLL and N³LL result respectively, and the dotted-black line is the N³LL result without δE_{21}^{us} . *Lower right panel:* Comparison of the $\nu_f = 2$ GeV (green), $\nu_f = 1$ GeV (orange) and $\nu_f = 0.7$ GeV (black) lines. For each case, the dashed line is the N³LO result and the solid line the N³LL one.

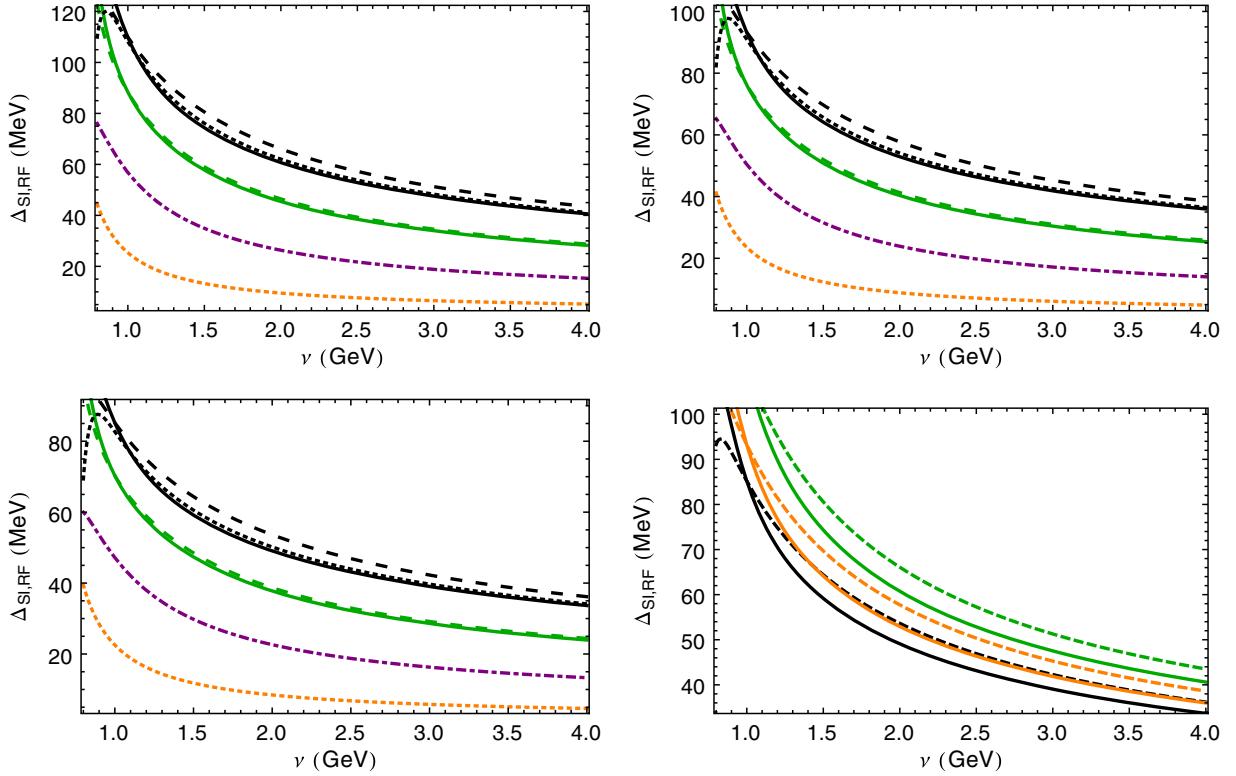


FIG. 4. Plots for $\Delta_{SI}^{(B_c)} - \Delta_{SI}^{(bb)}/2 - \Delta_{SI}^{(cc)}/2$ in the RS' scheme with $\nu_{us} = 1$ GeV. *Upper left, upper right and bottom left panels:* Plots for $\nu_f = 2, 1$ and 0.7 GeV respectively. The orange-dotted, purple dot-dashed, green-dashed and black-dashed lines are the LO-N³LO results respectively. The solid-green and solid-black lines are the NNLL and N³LL result respectively, and the dotted-black line is the N³LL result without δE_{21}^{us} . *Bottom right panel:* Comparison of the $\nu_f = 2$ GeV (green), $\nu_f = 1$ GeV (orange) and $\nu_f = 0.7$ GeV (black) lines. For each case, the dashed line is the N³LO result and the solid line the N³LL one.

this gave a reasonable estimate. Such value and the experimental masses of bottomonium and charmonium yields $\Delta_{SI}^{(B_c)} - \Delta_{SI}^{(bb)}/2 - \Delta_{SI}^{(cc)}/2 \sim 60$ MeV.

B. Fine splitting

The $E(1^3P_j) - E(1^3P_{j'})$ energy differences are interesting objects for study, they are free of renormalon effects (we take $\nu_f = 1$ GeV for reference but the result is quite insensitive to this) and also of ultrasoft effects. In this paper, we have obtained, for the first time, theoretical expressions with relative NLL precision (i.e., we have two terms of the weak-coupling expansion and we also know the RGI expression for them). We would like to see how well our theoretical predictions compare with experiment.

We first start with bottomonium, which, in principle, is the system where the weak-coupling approach should work better. We plot the strict weak-coupling predictions in Fig. 5. We expect the large logarithms to be resummed around $\nu \sim$ soft scale, of order 1 GeV. Indeed, we observe a much better agreement at those scales, and results compatible with experiment, assuming that the relative size of the uncomputed $\mathcal{O}(m\nu^6)$ corrections is of order 20%–30%. We also observe that the resummation of (hard) logarithms

produces a sizable effect but of the order of uncertainties. At those scales we also observe convergence of the expansion (the N³LL correction is smaller than the NNLL correction). If we repeat the analysis for charmonium the numbers we get are quite low when compared with experiment. We show them in Fig. 6. In principle, this confirms the expectation that charmonium *P*-wave states can not be described by a weak-coupling analysis. For completeness, we also show the prediction of the strict weak-coupling analysis for the fine splitting of the *P*-wave B_c states in Fig. 7.

We also study the ratio

$$\begin{aligned} \rho &= \frac{E(1^3P_2) - E(1^3P_1)}{E(1^3P_1) - E(1^3P_0)} \\ &= \frac{4}{5} + \frac{6(m_1 - m_2)^2}{5(m_1^2 + 10m_1m_2 + m_2^2)} + \mathcal{O}(\alpha_s). \end{aligned} \quad (5.4)$$

One can speculate that this observable is cleaner in the sense that the NR matrix element cancels in the ratio at the leading nonvanishing order. Nevertheless, this observable is also sensitive to the wave function at the next order. We show the result in Fig. 8. There is a difference with

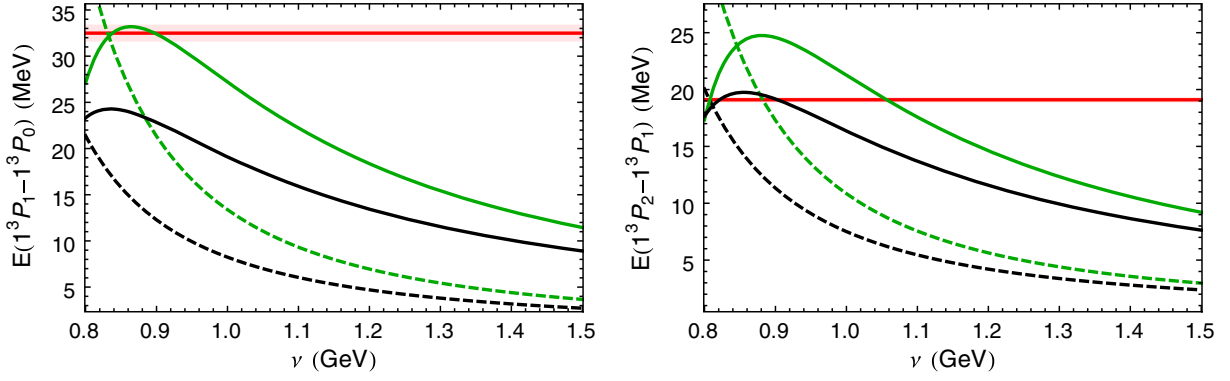


FIG. 5. Plots for the P -wave fine splittings in bottomonium in the RS' scheme with $\nu_f = 1$ GeV and $\nu_h = m_{b,RS'}$. The red band is the experimental value. The dashed-green, dashed-black, solid-green, and the solid-black lines are the NNLO, NNLL, N^3LO and N^3LL results respectively. *Left panel:* Plot of $M_{\chi_{b1}} - M_{\chi_{b0}}$. *Right panel:* Plot of $M_{\chi_{b2}} - M_{\chi_{b1}}$.

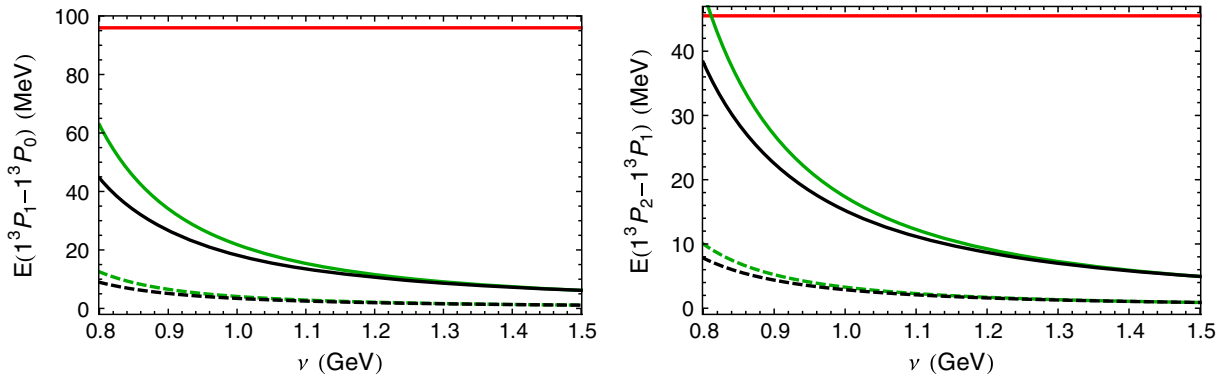


FIG. 6. Plots for the P -wave fine splittings in charmonium in the RS' scheme with $\nu_f = 1$ GeV and $\nu_h = m_{c,RS'}$. The red band is the experimental value. The dashed-green, dashed-black, solid-green, and the solid-black lines are the NNLO, NNLL, N^3LO and N^3LL results respectively. *Left panel:* Plot of $M_{\chi_{c1}} - M_{\chi_{c0}}$. *Right panel:* Plot of $M_{\chi_{c2}} - M_{\chi_{c1}}$.

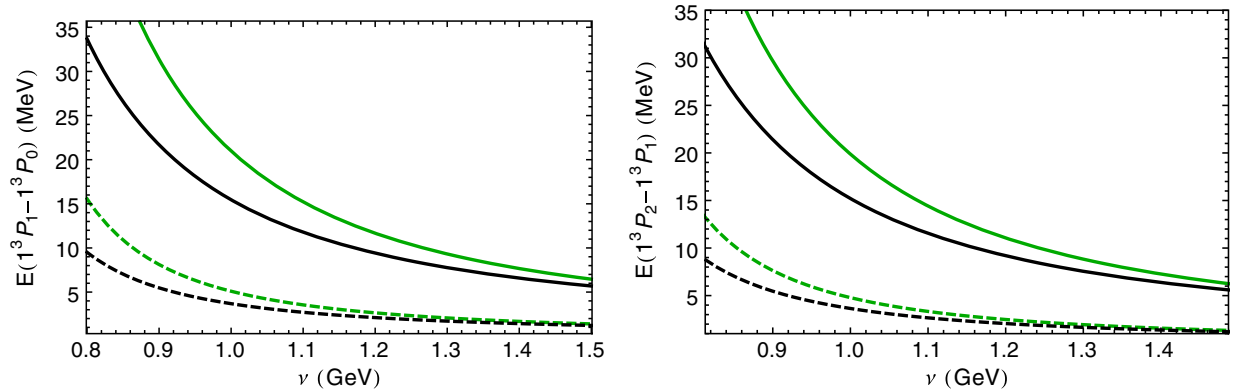


FIG. 7. Plots for the P -wave fine splitting in B_c in the RS' scheme with $\nu_f = 1$ GeV and $\nu_h = 2m_{b,RS'}m_{c,RS'}/(m_{b,RS'} + m_{c,RS'})$. The dashed-green, dashed-black, solid-green, and the solid-black lines are the NNLO, NNLL, N^3LO and N^3LL results respectively. *Left panel:* Plot of $M_{B_c(1^3P_1)} - M_{B_c(1^3P_0)}$. *Right panel:* Plot of $M_{B_c(1^3P_2)} - M_{B_c(1^3P_1)}$.

experiment of order 25%. The resummation of hard logarithms does not improve the agreement with data (it actually makes it slightly worse, specially for the LL result). The difference between theory and experiment in

the case of charmonium is larger, since the theoretical prediction is more or less equal as for bottomonium but the experimental value of ρ is significantly different for bottomonium and charmonium. For completeness, we also

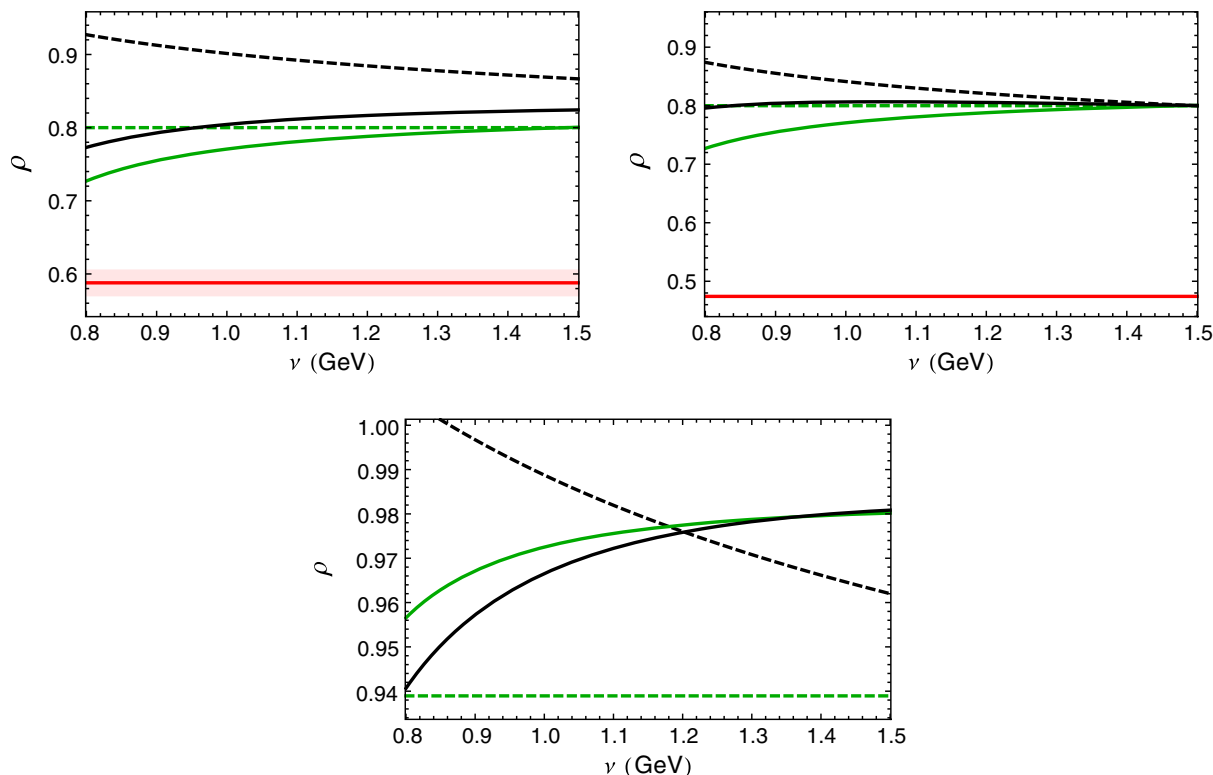


FIG. 8. Plots of ρ expanded in powers of α_s in the RS' scheme with $\nu_f = 1$ GeV. The red line is the experimental value. We start the counting at the leading nonvanishing order. Then, the dashed-green, dashed-black, solid-green, and solid-black lines are the LO, LL, NLO and NLL results respectively. *Upper left panel:* Plot for bottomonium with $\nu_h = m_{b,RS'}$. *Upper right panel:* Plot for charmonium with $\nu_h = m_{c,RS'}$. *Bottom panel:* Plot for B_c with $\nu_h = 2m_{b,RS'}m_{c,RS'}/(m_{b,RS'} + m_{c,RS'})$.

show the prediction of the strict weak-coupling analysis of ρ for the B_c states. Note that, in this case, the leading-order theoretical prediction is different to the equal mass case [cf. Eq. (5.4)]. This provides an extra motivation to measure this ratio.

C. Hyperfine splitting

Finally, we consider the hyperfine splitting of the P -wave states. We show our results in Fig. 9. The strict weak-coupling prediction of the hyperfine splitting is perfectly compatible with experiment. The resummation of (hard) logarithms is a tiny effect and does not affect this conclusion. Surprisingly enough, this is also true for charmonium (then we conjecture that the prediction we give for the P -wave B_c , compatible with zero, is also robust). This could be accidental. The key issue for the agreement is that the expectation value of the relativistic potential is small. We elaborate on this issue in Sec. VII.

VI. ALTERNATIVE COUNTING APPROACH

In the previous section, we have confronted the strict weak-coupling theoretical predictions with the experimental values of the masses of the $n = 2, l = 1$ excitations for

bottomonium, charmonium and B_c . For bottomonium, the convergence was somewhat marginal. On the other hand the predictions were consistent with experiment (for the ρ ratio the situation was somewhat worse but still consistent with the expected size of higher-order relativistic corrections). For charmonium and B_c the situation was significantly worse. Only for the hyperfine case there was agreement with experiment.

We now study a computational scheme that reorganizes the perturbative expansion such that it performs a selective sum of higher-order corrections (such scheme was already applied in [27–29]). We want to test if such scheme could improve/accelerate the convergence. In this method, we incorporate the static potential exactly (to a given order) in the leading-order Hamiltonian (the explicit ν dependence of the static potential appears at N³LO and partially cancels with the explicit ν dependence of Eq. (3.6), the ultrasoft correction):

$$\left[\frac{\mathbf{p}^2}{2m_r} + V_{N,RS'}^{(0)}(r; \nu) \right] \phi_{nl}^{(0)}(\mathbf{r}) = E_{nl}^{(0)} \phi_{nl}^{(0)}(\mathbf{r}), \quad (6.1)$$

where the static potential will be approximated by a polynomial of order $N + 1$,

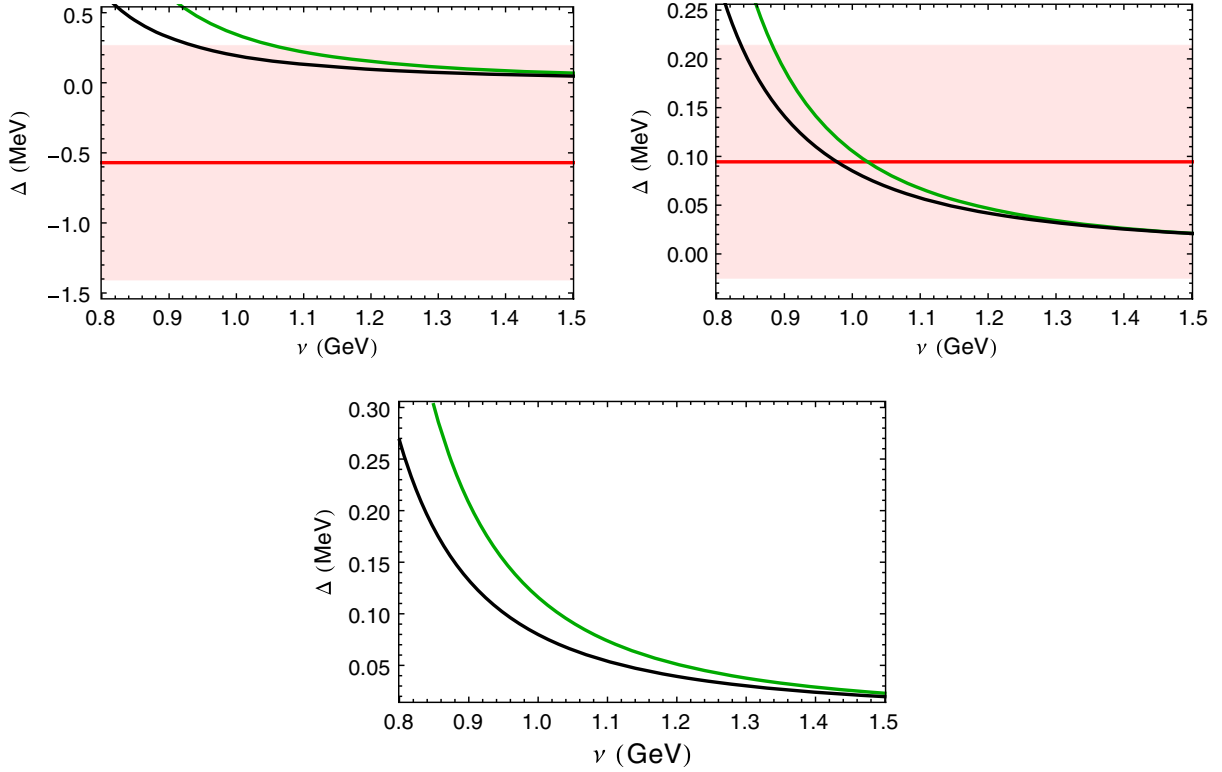


FIG. 9. Plots for the P -wave hyperfine splitting Δ in the RS' scheme with $\nu_f = 1$ GeV. The red line is the experimental value, the solid-green line the N^3LO result and the solid-black line is the N^3LL result. *Upper left panel:* Plot for bottomonium with $\nu_h = m_{b,RS'}$. *Upper right panel:* Plot for charmonium with $\nu_h = m_{c,RS'}$. *Lower panel:* Plot for B_c with $\nu_h = 2m_{b,RS'}m_{c,RS'}/(m_{b,RS'} + m_{c,RS'})$.

$$V_{N,RS'}^{(0)}(r; \nu) = \begin{cases} (V_N^{(0)} + 2\delta m_{RS'}^{(N)})|_{\nu=\nu} \equiv \sum_{n=0}^N V_{RS',n} \alpha_s^{n+1}(\nu) & \text{if } r > \nu_r^{-1} \\ (V_N^{(0)} + 2\delta m_{RS'}^{(N)})|_{\nu=1/r} \equiv \sum_{n=0}^N V_{RS',n} \alpha_s^{n+1}(1/r) & \text{if } r < \nu_r^{-1}. \end{cases} \quad (6.2)$$

$V_N^{(0)}$ is the static potential defined in Eq. (A1). We implement the renormalon cancellation working in the RS' scheme. Expressions for $\delta m_{RS'}$ can be found in Ref. [27]. In principle, we would like to take N as large as possible (though we also want to explore the dependence on N). In practice, we take the static potential at most up to $N = 3$, i.e., up to $\mathcal{O}(\alpha_s^4)$. This is the order to which the coefficients $V_{RS',n}$ are completely known.

Taking different values for ν_r and ν_f in Eq. (6.2), we obtain the most relevant limits:

(a) The case $\nu_r = \infty$, $\nu_f = 0$ is nothing but the on-shell static potential at fixed order, i.e., Eq. (A1). Note that the $N = 0$ case reduces to a standard computation with a Coulomb potential, for which we can compare with analytic results for the matrix elements. We use this fact to check our numerical solutions of the Schrödinger equation.

(b) The case $\nu_r = \infty$ (with finite nonzero ν_f) is nothing but adding an r -independent constant to the static potential.

(c) The case $\nu_r = \text{finite}$ (and, for consistency, $\nu_r \geq \nu_f$). We expect this case to improve over the previous results, as it incorporates the correct (logarithmically modulated) short distance behavior of the potential. This has to be done with care in order not to spoil the renormalon cancellation. For this purpose it is compulsory to keep a finite, nonvanishing, ν_f , otherwise the renormalon cancellation is not achieved order by order in N , as it was discussed in detail in Ref. [55].

We have explored the effect of different values of ν_f in our analysis. Large values of ν_f imply a large infrared cutoff. In this way, our scheme becomes closer to an \overline{MS} -like scheme. Such schemes still achieve renormalon cancellation, yet they jeopardize the power counting, as the

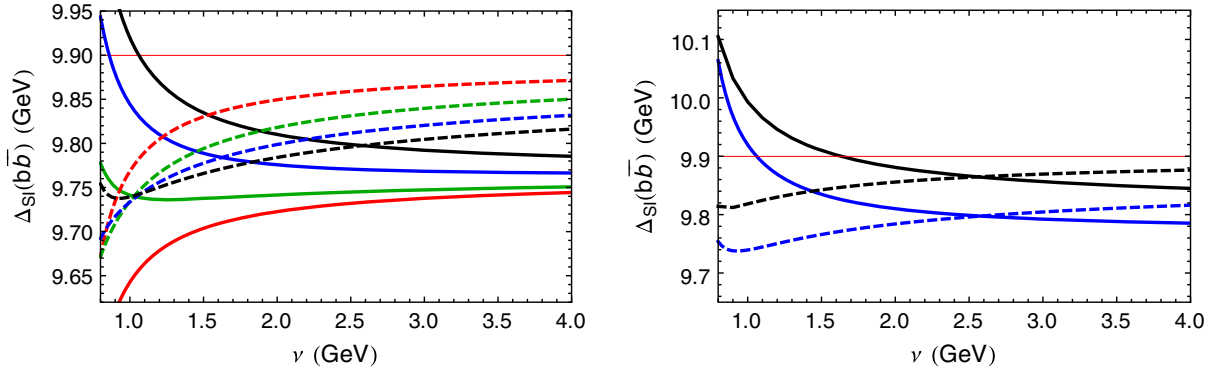


FIG. 10. *Left panel:* Plot of $2m_b + E_{21}^{(0)}$ for bottomonium using $V_{N,RS'}^{(0)}$ for $N = 0$ (red), 1 (green), 2 (blue), 3 (black). Dashed lines are computed with $\nu_f = 0.7$ GeV and continuous lines with $\nu_f = 1$ GeV. *Right panel:* Plot of $2m_b + E_{21}^{(0)}$ for bottomonium using $V_{N,RS'}^{(0)}$ for $N = 3$. Dashed lines are computed with $\nu_f = 0.7$ GeV and continuous lines with $\nu_f = 1$ GeV. Blue lines correspond to the black lines of the left panel. Black lines are computed at strict weak coupling.

residual mass $\delta m_{RS'}$ does not count as mv^2 . As a consequence, consecutive terms of the perturbative series become bigger. Therefore, we prefer values of ν_f as low as possible, with the constraints that one should still obtain the renormalon cancellation, and that it is still possible to perform the expansion in powers of α_s .

The energy $E_{nl}^{(0)}$ in Eq. (6.1) correctly incorporates the N^N LO corrections to the spectrum associated to the static potential. It also includes higher-order corrections (those generated by the iteration of the static potential). In order for this computational scheme to make sense, it first requires that the $N \rightarrow \infty$ converges, or at least that the error is small compared with the relativistic correction. We show the result of the computation of $E_{21}^{(0)}$ for bottomonium in Fig. 10 setting $\nu_r = \infty$ (setting $\nu_r = 1$ GeV does not change the qualitative picture) and $\nu_f = 1$ or 0.7 GeV. We do not see convergence for $\nu_f = 1$ GeV but we get it for $\nu_f = 0.7$ GeV. Either way, it is worth emphasizing that, for $N = 3$, the $\nu_f = 1$ and 0.7 GeV are consistent with each other, as we can see in Fig. 10 (left). This shows a mild dependence on ν_f . On the other hand, the dependence on ν is still large. We can also compare with the strict weak-coupling expansion result. We do so in Fig. 10 (right). We find a difference of order 60 MeV. This difference appears to be very stable under ν or ν_f variations. The origin of this constant shift is not clear to us at present. Setting $\nu_r = 1$ GeV does not qualitatively change the picture. Overall, we take $E_{nl}^{(0)} \sim 9.8$ GeV as the leading $\mathcal{O}(v^2)$ solution. Note that this number still suffers from sizable uncertainties ($\sim \pm 60$ MeV if looking to the scale variation or the difference with the strict weak-coupling evaluation).

Once we have the leading $\mathcal{O}(v^2)$ solution, we can consider the incorporation of the relativistic and ultrasoft corrections, which will scale, at most, as $\mathcal{O}(v^4)$. With the accuracy of this work, we only have to take the expectation value of δV where

$$\delta V = V_s - V^{(0)} \quad (6.3)$$

stands for the relativistic potential (V_s is the total singlet potential) that contributes up to N^3 LL and also add the ultrasoft correction from Eq. (3.6). Overall the mass of the bound states reads

$$M(n, l, j) = m_1 + m_2 + E_{nl}^{(0)} + {}^{(0)}\langle n, l | \delta V | n, l \rangle^{(0)} + \delta E_{nl}^{\text{us}}, \quad (6.4)$$

where $E_{nl}^{(0)}$ counts as v^2 , ${}^{(0)}\langle n, l | \delta V | n, l \rangle^{(0)}$ counts as v^4 (including also $v^4 \alpha_s$ corrections) and $\delta E_{nl}^{\text{us}}$ as v^5 . Eq. (6.4) is numerically correct with N^3 LL precision and incorporates extra subleading terms (albeit in an incomplete way). If one sets $\nu_h = \nu_{\text{us}} = \nu$ one also recovers the N^3 LO result incorporating some extra subleading terms. For notation purposes we will label the results obtained using Eq. (6.4) as N^i LL(N) where N stands for the order at which the static potential (we introduce exactly in the Schrödinger equation) is truncated and i will be 2 or 3 depending on the order at which the relativistic and ultrasoft corrections are included. A similar counting will apply to the N^i LO(N) result, where we do not perform the logarithmic resummation by setting $\nu_h = \nu_{\text{us}} = \nu$.

Note that the correction to the static potential generated by the resummation of ultrasoft logarithms obtained in Eq. (2.8) is not incorporated in Eq. (6.2) but rather added to Eq. (6.3) as part of the correction.⁷

Overall, this computational scheme resums a subset of subleading corrections in the hope that they would account for the bulk of such subleading terms. This could be so if the higher-order corrections that we infer from our

⁷Adding Eq. (2.8) to Eq. (6.2) would redefine the leading $\mathcal{O}(v^2)$ solution. We do not explore this line of research in this paper.

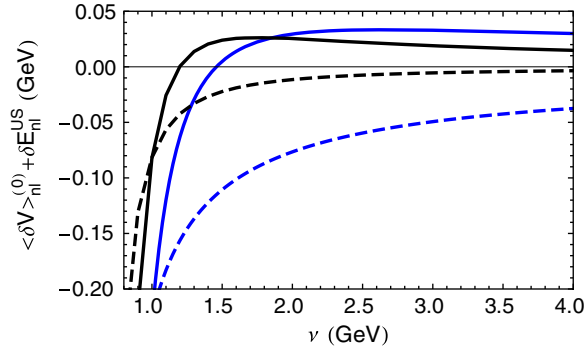


FIG. 11. Plot of the $\langle \delta V \rangle_n^{(0)} + \delta E_n^{US}$ contribution to Δ_{SI} for bottomonium with N³LL (continuous black line), N³LL(3) (continuous blue line), N³LO (dashed black line), N³LO(3) (dashed blue line) precision, evaluated with $\nu_r = \infty$ GeV, $\nu_f = 1$ GeV, $\nu_{us} = 1$ GeV. Alternative plots with $\nu_r = 1$ GeV or $\nu_f = 0.7$ GeV change little.

knowledge of the static potential are indeed responsible for the leading corrections.

The expressions we use for the relativistic potential (valid also in the unequal mass case) are taken from Ref. [6], which uses the computation of the $1/m$ potential obtained in Ref. [56]. For ease of reference we quote them in Appendix A. We can use any of the bases for the potentials presented in that paper, which were referred as: Wilson, onshell, Coulomb or Feynman. At strict N³LO they all yield the same result. Since the computational scheme we implement in this section partially resums higher orders some dependence on the basis of potentials shows up. We have checked that, for the set of bases we consider, the dependence is quite small.

The computation of the relativistic corrections opens new issues compared with the static potential. In the case of the static potential, the natural scale is $\nu \sim 1/r$, except in the $\mathcal{O}(\alpha_s^4)$ term where also the ultrasoft scale ν_{us} appears.⁸ The case of the relativistic potentials is quite different. They are much more dependent on the hard, and above all, the ultrasoft scale (on the other hand they are formally insensitive to the pole mass renormalon). Moreover, in order for the computation with the static potential to be a more or less reasonable approximation we need to have at least three or more terms (also important is the resummation of soft logarithms). For the case of the relativistic potentials, we have at most two terms. This, together with a much stronger scale dependence, can trigger that inefficiencies of the description of the relativistic potentials get amplified when computing the expectation values. In this respect, for the first time, we have two terms of the perturbative expansion of the (relativistic) potentials, for which the complete resummation of large logarithms is

⁸If one considers the RGI expression ultrasoft logs already appear at $\mathcal{O}(\alpha_s^3)$.

known. This allows us to compare fixed-order with RGI results. We do this comparison in Fig. 11. We observe that the resummation of logarithms happens to be crucial to get consistent results between the strict and the alternative counting scheme. It makes the correction much smaller too (which is good news for the validity of the velocity expansion), and, as we will see next, it helps in getting reasonable agreement with experiment.

VII. PHENOMENOLOGY: $n=2, l=1$. ALTERNATIVE COUNTING APPROACH

We now repeat the analysis of Sec. V but using the predictions obtained in the previous section. We first plot our prediction of Δ_{SI} in Fig. 12. The bulk of the difference with the strict weak-coupling computation comes from the different results of the static solution. On the other hand, the relativistic corrections are similar. We emphasize again that for this to be the case, the resummation of large logarithms is crucial. The final result is compatible with experiment within uncertainties.

We now turn to the fine splittings. We remark that they are renormalon-free observables. Indeed, the results are virtually insensitive to ν_f , so by default we will use $\nu_f = 1$ GeV. Therefore, they are a cleaner place than $E_{21}^{(0)}$ to test the convergence of truncating at N the static potential. We show such plot in Fig. 13 (left). In the left figures, we plot the fine splitting with NNLO(N) accuracy. This figure effectively draws (up to a constant) $\langle 1/r^3 \rangle_{21}$ for bottomonium using different N 's, which allows us to check the convergence associated to the static potential. The convergence is somewhat marginal. Things improve considerably when we include higher-order corrections to the NNLO(3) result. We show the results in Fig. 13 (right). Moving from NNLO(3) to NNLL(3) (incorporating the resummation of large hard logarithms) makes the result more scale independent and closer to experiment. Going to N³LL(3) or N³LO(3) improves the result. They are quite scale independent, quite close among them, and in quite good agreement with experiment. For $E(1^3P_1) - E(1^3P_0)$ the N³LL(3) theoretical result hits the experimental value at the scale of minimal sensitivity. For $E(1^3P_2) - E(1^3P_1)$, the N³LL(3) theoretical result is around 5 MeV above the experimental value at the scale of minimal sensitivity. Overall, the agreement with experiment is quite remarkable. If we compare with the strict weak-coupling results, they typically yield smaller values than the alternative computational approach, and show a larger factorization scale dependence. Nevertheless, the N³LO and N³LL results in the strict weak-coupling approximation are in reasonable agreement with the N³LO(3) and N³LL(3) result obtained in this alternative computational approach at the scale of minimal sensitive of both. If we look to the difference between the NNLL(3) and N³LL(3) the difference is small. On the other hand the difference between

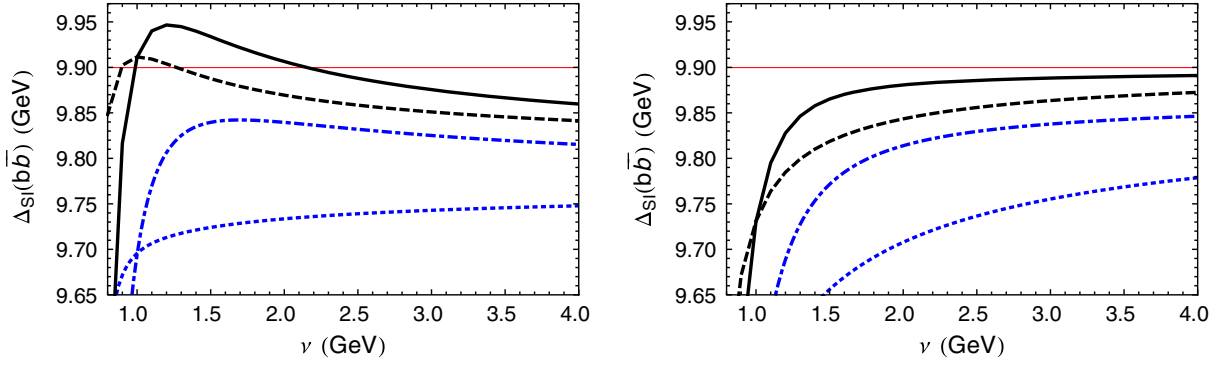


FIG. 12. Plot of Δ_{SI} evaluated with N^3LL (continuous black line), $N^3LL(3)$ (dash-dotted blue line), N^3LO (dashed black line) and $N^3LO(3)$ (dotted blue line) precision. All lines are computed with $\nu_r = \infty \text{ GeV}$ and $\nu_{us} = 1 \text{ GeV}$ and *Left panel* with $\nu_f = 1 \text{ GeV}$ and *Right panel* with $\nu_f = 0.7 \text{ GeV}$.

NNLO(3) and $N^3LO(3)$ is bigger. In both cases, they converge to experimental value.

Note that the $N^3LO/LL(N)$ result is the sum of a $N^3LO/LL(N)$ contribution coming from the potential and a $N^3LO/LL(N)$ contribution coming from the NRQCD

Wilson coefficients, neglecting crossed terms, which are subleading.

We now consider the hyperfine splitting, Δ , defined in Eq. (4.6). It starts giving a nonzero contribution at N^3LO/N^3LL . This observable is sensitive to $\langle \text{reg} \frac{1}{\bar{s}} \rangle$ (the

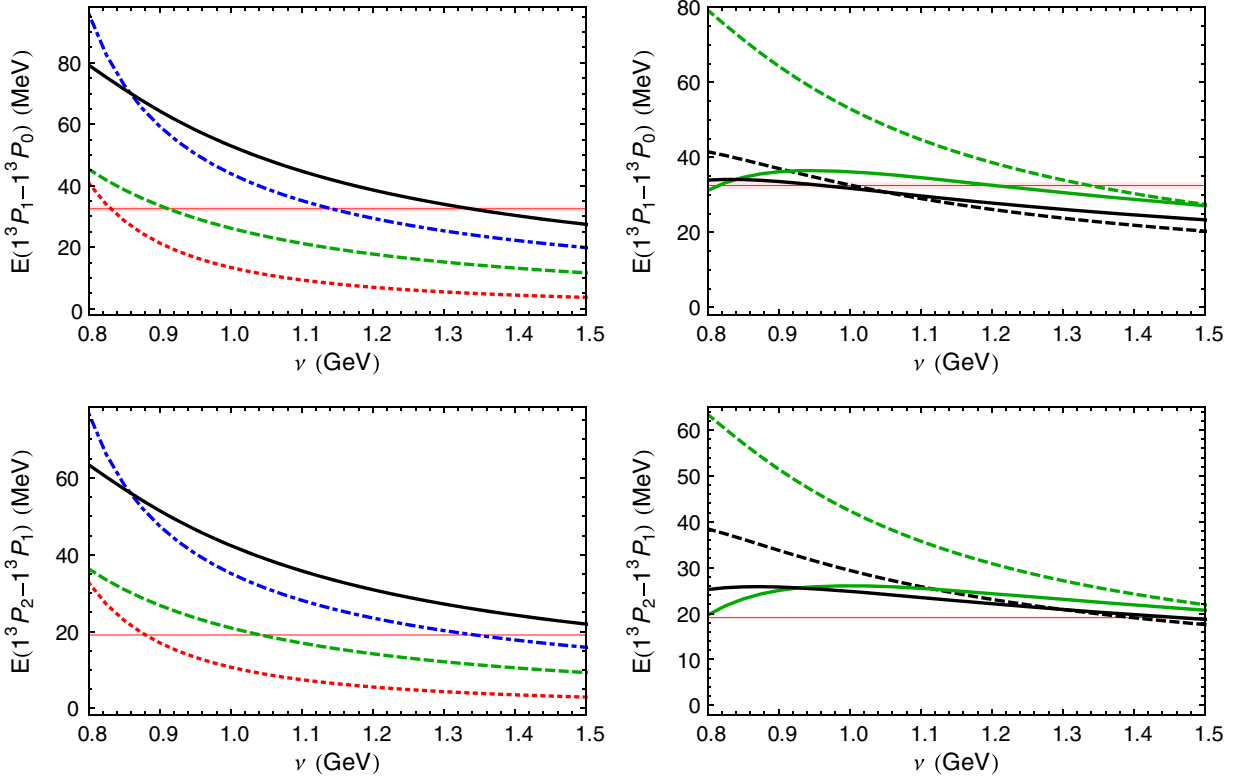


FIG. 13. Plots for the P -wave fine splittings in bottomonium in the RS' scheme with $\nu_f = 1 \text{ GeV}$ and $\nu_h = m_{b,RS'}$. Red band is the experimental value. *Left-up panel*: Plot of $E(1^3P_1) - E(1^3P_0)$ with NNLO(N) accuracy with $N = 0$ (dotted red line), 1 (dashed green line), 2 (dash-dotted blue line), 3 (continuous black line). *Left-bottom panel*: Plot of $E(1^3P_2) - E(1^3P_1)$ with NNLO(N) accuracy with $N = 0$ (dotted red line), 1 (dashed green line), 2 (dash-dotted blue line), 3 (continuous black line). *Right-up panel*: Plot of $E(1^3P_1) - E(1^3P_0)$ with NNLO(3) accuracy (dashed green line), NNLL(3) accuracy (dashed black line), $N^3LO(3)$ accuracy (continuous green line) and $N^3LL(3)$ accuracy (continuous black line). *Right-bottom panel*: Plot of $E(1^3P_2) - E(1^3P_1)$ with NNLO(3) accuracy (dashed green line), NNLL(3) accuracy (dashed black line), $N^3LO(3)$ accuracy (continuous green line) and $N^3LL(3)$ accuracy (continuous black line).

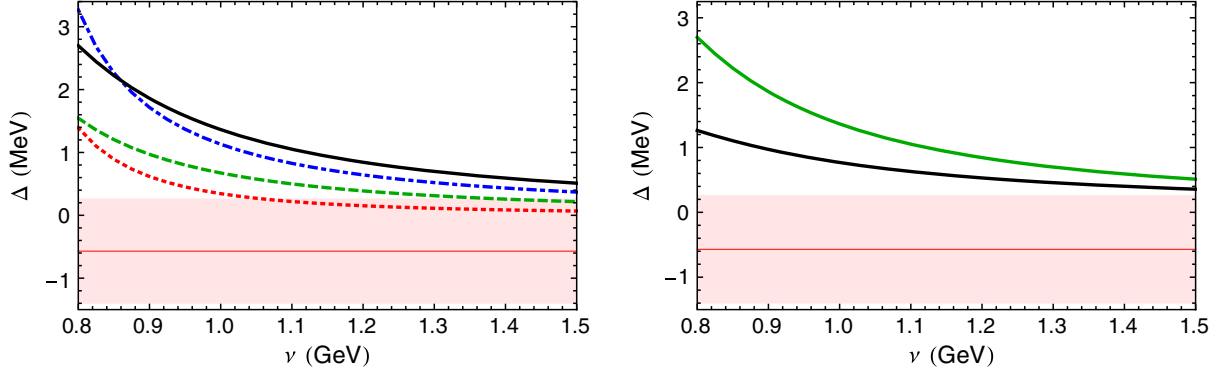


FIG. 14. Plots of Δ , the hyperfine splitting for P -wave bottomonium, in the RS' scheme with $\nu_f = 1$ GeV and $\nu_h = m_{b,RS'}$. Red band is the experimental value. *Left panel:* Plot of Δ with $N^3LO(N)$ accuracy with $N = 0$ (dotted red line), 1 (dashed green line), 2 (dash-dotted blue line), 3 (continuous black line). *Right panel:* Plot of Δ with $N^3LO(3)$ accuracy (continuous green line) and $N^3LL(3)$ accuracy (continuous black line).

N^3LO and N^3LL expression for the fine splitting is also sensitive to the matrix element of this operator). We can then check the convergence in N by computing the $N^3LO(N)$ result (i.e., the matrix element) for different N 's. We show the outcome in the left panel of Fig. 14. The convergence is similar to the fine case. Corrections are large and so is the ν scale dependence. The resummation of the hard logarithms improve the agreement with experiment, still the strict weak-coupling result shows a better agreement with experiment. In the above computation, we only have the first term of the perturbative expansion in the strict weak-coupling limit. We conjecture that higher-order terms of the relativistic potential will compensate this behavior. In other words, we do not know the shape of the relativistic corrections with enough accuracy at short distances. This introduces large errors when producing expectation values of them. In this respect, it is interesting to see what lattice simulations can add to this discussion. The hyperfine splitting is specially clean, as it only depends on V_{S^2} . Indeed, for P -wave states, any dependence on the delta potential vanishes and only the r dependence (at nonzero r) is relevant. Lattice determinations of V_{S^2} were obtained in [57,58]. In the first reference, the lattice simulations were basically compatible with zero (up to a lattice version of $\delta(\mathbf{r})$, which obviously does not contribute to the hyperfine). The second reference gives a parametrization which has a nontrivial r dependence (with no delta potential). This could give a large contribution to the hyperfine splitting and, thus, making the theoretical prediction incompatible with the experimental figure, which is approximately zero.⁹

Finally we study ρ ratio. We show our results in Fig. 15. The $LO(N)$ and $LL(N)$ results are equal (for any N) to the strict weak-coupling computation. For the $NLO(3)$ and

$NLL(3)$ results, we consider two options: Directly considering the ratio between the energy differences or treating the $\mathcal{O}(\alpha_s)$ correction to the relativistic potential perturbatively. At small scales the difference between both approaches becomes significant, specially for the $NLO(3)$ result, which approaches the experimental result. At present, the spread of values depending on the truncation does not allow us to reach definite conclusions. Differences with experiment are of order 20%, in principle achievable with higher-order corrections.

The issues discussed above deserve further dedicated studies. Indeed, to settle (some of) them, it would be very interesting to compute the next correction in the weak-coupling expansion of the relativistic potential that contributes to this observable. This is a complicated task but within reach. Indeed, for the future, the fine and hyperfine splittings are ideal candidates for dedicated analyses aiming at $\mathcal{O}(mv^6)$ precision. This is in principle feasible, and may lead to precise predictions with small errors.

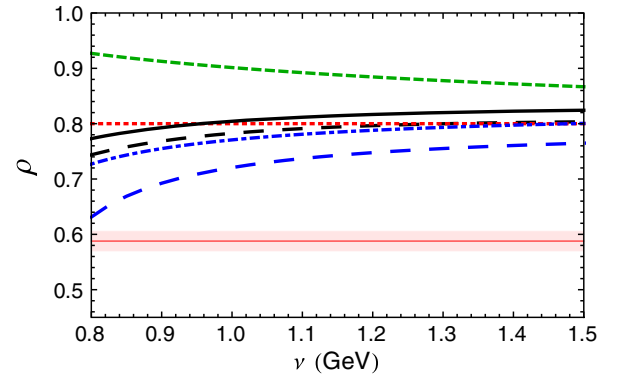


FIG. 15. Plot of ρ for bottomonium. We plot the $LO = LO(N)$ (dotted red line), $LL = LL(N)$ (dashed green line), $NLO(3)$ (dot-dashed blue line) and $NLL(3)$ (solid black line) results (the latter two treating the $\mathcal{O}(\alpha_s)$ correction to the relativistic potential perturbatively). The $NLO(3)$ and $NLL(3)$ result from the energy differences are the long-dashed blue and black lines respectively.

⁹Nevertheless, it is not that clear whether the lattice simulations of [58] at short distances cannot indeed be parametrized by a delta potential. A.P. acknowledges discussions with Gunnar Bali on this point.

VIII. CONCLUSIONS

In this paper, the P -wave heavy quarkonium spectrum has been obtained for the first time at strict weak coupling with $N^3\text{LL}$ precision. We have obtained such precision for the equal and nonequal mass cases and for the fine and hyperfine splittings as well. We emphasize that these results also give the $\mathcal{O}(m\alpha_s^6 \ln(1/\alpha_s))$ correction to the spectrum (for P -wave states) for the first time. Remarkably, the results we obtain are compatible with experiment, for $n = 2$, $l = 1$ bottomonium, albeit with large uncertainties. For the spin-independent energy combination Δ_{SJ} , defined in Eq. (5.1), the convergence is somewhat marginal. For the fine splitting, approximate agreement can be found at scales of around 1 GeV, also for the hyperfine. In any case, the uncertainties are large, to the point that the incorporation of the resummation of logarithms produces energy shifts which are inside the expected uncertainties. For charmonium and B_c we have also performed exploratory studies. We found that the scale dependence is larger and the convergence worse. At this stage we refrain of trying quantitative analyses of these states.

For Δ_{SJ} , the $N^3\text{LL}$ result is the maximal accuracy (in analytic terms) that can be obtained in the foreseeable future. For some specific (the fine and hyperfine) energy splittings, it is still within reach (with a quite significant, but finite, amount of effort) to go further analytically, and obtain the complete $\mathcal{O}(m\alpha_s^6)$ result (or its RGI expression, which however could be much more difficult). This implies computing the $\mathcal{O}(v^2)$ corrections to the leading nonvanishing term. It would give a hint of the size of the relativistic corrections, which is quite compelling. We have already seen that present evaluations of the ρ -ratio of the fine splittings are off by around 25%, even though the description of the individual energy splittings is quite reasonable. It would be interesting to see the impact of the incorporation of the $\mathcal{O}(v^2)$ corrections to this specific observable. For the case of the hyperfine splitting at present only the leading nonvanishing term is known. The present evaluation agrees with experiment. Therefore, it is of great interest to check if such agreement survives the incorporation of higher-order corrections. Leaving aside these energy differences, going beyond $N^3\text{LL}$ would require to go to $N^4\text{LO}$. For the gross spectrum, Δ_{SJ} , this would require the much demanding computation of the static potential with four-loop accuracy, other necessary computations would also be quite difficult.

In view of the difficulty of obtaining complete higher-order corrections, one will have to rely on approximations. The first one, which we have already applied here, explores selective resummations of higher-order corrections. We incorporate the static potential (truncated to a given power in α_s) exactly in the Schrödinger equation [see Eq. (6.1)]. We take the result as the leading $\mathcal{O}(v^2)$ term. In order for

this approach to be sensible, this leading $\mathcal{O}(v^2)$ term has to be more or less stable when truncating at different orders in the static potential (for large N). With $\nu_f = 1$ GeV we do not get a convergent pattern, though we get it for $\nu_f = 0.7$ GeV, and both results are relatively close for $N = 3$ (as long as the scale ν is not very small). We observe that, compared with the strict weak-coupling computation, we find an almost constant shift downwards of order ~ 60 MeV. At this point we do not have a clear explanation for this fact, and only speculate that it may have to do with inefficiencies in the renormalon cancellation in the static potential. Leaving this problem aside, we consider the incorporation of the relativistic corrections. These are renormalon-free quantities but much more sensitive to the hard, and above all, the ultrasoft scales. We can make interesting observations. If we consider the relativistic corrections to the energy without logarithmic resummation, we observe that they yield quite different results in the alternative counting versus the strict weak-coupling computation. The former generates a much bigger correction that deteriorates the agreement with data. Remarkably, the resummation of logarithms fixes this problem. After the resummation of logarithms both the strict weak-coupling computation and the alternative counting scheme yield consistent results for the relativistic corrections of Eq. (5.1).

We also apply this alternative counting scheme to the fine and hyperfine. They are free of renormalon and ultrasoft effects. Therefore, they are potentially rather clean observables. Also interesting observations can be made here. The convergence of the static solution is still slow. Nevertheless, a rather reasonable agreement with experiment is obtained for the fine splittings after inclusion of the $\mathcal{O}(\alpha_s)$ corrections to the potential. For the ρ ratio, however, the situation is somewhat inconclusive and so is for the hyperfine splitting. We conjecture that higher-order perturbation corrections can be important to obtain precise predictions for these observables.

ACKNOWLEDGMENTS

This work was supported in part by the Spanish grants FPA2014-55613-P, FPA2017-86989-P and SEV-2016-0588. J. S. acknowledges the financial support from the European Union's Horizon 2020 research and innovation programme under the Marie Skłodowska-Curie Grant Agreement No. 665919, and from Spanish MINECO's Juan de la Cierva-Incorporación programme, Grant Agreement No. IJCI-2016-30028.

APPENDIX A: THE POTENTIAL

We display here the $\overline{\text{MS}}$ renormalized expressions for the NRQCD potentials necessary to compute the $N^3\text{LO}$ spectrum. The static potential reads

$$V_N^{(0)}(r; \nu) = -\frac{C_F \alpha_s(\nu)}{r} \left\{ 1 + \sum_{n=1}^N \left(\frac{\alpha_s(\nu)}{4\pi} \right)^n a_n(\nu; r) \right\}. \quad (\text{A1})$$

For the seaked N³LO precision one can truncate at $N = 3$ and the coefficients read

$$\begin{aligned} a_1(\nu; r) &= a_1 + 2\beta_0 \ln(\nu e^{\gamma_E} r), \\ a_2(\nu; r) &= a_2 + \frac{\pi^2}{3} \beta_0^2 + (4a_1 \beta_0 + 2\beta_1) \ln(\nu e^{\gamma_E} r) + 4\beta_0^2 \ln^2(\nu e^{\gamma_E} r), \\ a_3(\nu; r) &= a_3 + a_1 \beta_0^2 \pi^2 + \frac{5\pi^2}{6} \beta_0 \beta_1 + 16\zeta_3 \beta_0^3 + \left(2\pi^2 \beta_0^3 + 6a_2 \beta_0 + 4a_1 \beta_1 + 2\beta_2 + \frac{16}{3} C_A^3 \pi^2 \right) \ln(\nu e^{\gamma_E} r) \\ &\quad + (12a_1 \beta_0^2 + 10\beta_0 \beta_1) \ln^2(\nu e^{\gamma_E} r) + 8\beta_0^3 \ln^3(\nu e^{\gamma_E} r). \end{aligned} \quad (\text{A2})$$

The $\mathcal{O}(\alpha_s)$ term was computed in Ref. [59], the $\mathcal{O}(\alpha_s^2)$ in Refs. [60,61], the $\mathcal{O}(\alpha_s^3)$ logarithmic term in Ref. [62], the light-flavour finite piece in Ref. [63], and the pure gluonic finite piece in Refs. [64,65]. In the normalization used in this paper, specific expressions for the coefficients a_i can be found in Appendix A of Ref. [6].

The complete set of relativistic potentials in the on-shell scheme with N³LO accuracy were obtained in the equal mass case in Refs. [56,66] (for the NNLO result see Ref. [67]). For the unequal mass case (and for the specific renormalization scheme we use in this paper) they were computed in Ref. [6]. The resulting expressions read

$$\begin{aligned} \frac{V_{\text{on-shell}}^{(1,0)}(r)}{m_1} + \frac{V_{\text{on-shell}}^{(0,1)}(r)}{m_2} &= \frac{C_F^2 \alpha_s^2(e^{-\gamma_E}/r)}{2r^2} \frac{m_r}{m_1 m_2} \left(1 + \frac{\alpha_s}{2\pi} (a_1 - \beta_0) \right) \\ &\quad - \frac{C_F C_A \alpha_s^2(e^{-\gamma_E}/r)}{4m_r r^2} \left\{ 1 + \frac{\alpha_s}{\pi} \left(\frac{89}{36} C_A - \frac{49}{36} T_F n_f - C_F + \frac{4}{3} (C_A + 2C_F) \ln(\nu r e^{\gamma_E}) \right) \right\}. \end{aligned} \quad (\text{A3})$$

$$V_{\text{p}^2, \text{on-shell}}^{(2,0)}(r) = -\frac{C_F \alpha_s^2}{3\pi} \frac{1}{r} C_A \ln(\nu r e^{\gamma_E}), \quad (\text{A4})$$

$$V_{\text{p}^2, \text{on-shell}}^{(1,1)}(r) = -\frac{C_F \alpha_s(e^{-\gamma_E}/r)}{r} \left\{ 1 + \frac{\alpha_s}{4\pi} \left(a_1 + \frac{8}{3} C_A \ln(\nu r e^{\gamma_E}) \right) \right\}, \quad (\text{A5})$$

The spin-dependent and V_r potentials relevant for P -wave states can be found in Eqs. (2.19)–(2.24), Eq. (2.27) and Eq. (2.29). For a P -wave state, the equal mass case is trivially recovered by setting $m = m_1 = m_2$.

APPENDIX B: THE N³LO HEAVY QUARKONIUM SPECTRUM

In this Appendix, we collect the explicit expression for the fixed order N³LO P -wave spectrum. The P -wave spectrum at N³LO, was obtained in Ref. [4,5] for the equal mass case and in Ref. [6] for the unequal mass case. It reads

$$\begin{aligned} E_{\text{N}^3\text{LO}}(n, l, s, j) &= E_n^C \left(1 + \frac{\alpha_s}{\pi} P_1(L_\nu) + \left(\frac{\alpha_s}{\pi} \right)^2 P_2(L_\nu) \right. \\ &\quad \left. + \left(\frac{\alpha_s}{\pi} \right)^3 P_3(L_\nu) \right), \end{aligned} \quad (\text{B1})$$

$$P_1(L_\nu) = \beta_0 L_\nu + \frac{a_1}{2}, \quad (\text{B2})$$

$$P_2(L_\nu) = \frac{3}{4} \beta_0^2 L_\nu^2 + \left(-\frac{\beta_0^2}{2} + \frac{\beta_1}{4} + \frac{3\beta_0 a_1}{4} \right) L_\nu + c_2, \quad (\text{B3})$$

$$\begin{aligned} P_3(L_\nu) &= \frac{1}{2} \beta_0^3 L_\nu^3 + \left(-\frac{7\beta_0^3}{8} + \frac{7\beta_0 \beta_1}{16} + \frac{3}{4} \beta_0^2 a_1 \right) L_\nu^2 \\ &\quad + \left(\frac{\beta_0^3}{4} - \frac{\beta_0 \beta_1}{4} + \frac{\beta_2}{16} - \frac{3}{8} \beta_0^2 a_1 + 2\beta_0 c_2 + \frac{3\beta_1 a_1}{16} \right) L_\nu \\ &\quad + c_3, \end{aligned} \quad (\text{B4})$$

where $c_i = c_i^c + c_i^{nc}$, $L_\nu = \ln \frac{m\nu}{2C_F m_r \alpha_s} + S_1(n+l)$ and $E_n^C = -\frac{m_r C_F^2 \alpha_s^2}{2n^2}$. Expressions for c_2^c and c_3^c can be found in Eqs. (7.17) and (7.18) of Ref. [6] (see also Ref. [6] for definitions and notation);

$$c_2^{\text{nc}} = -\frac{2m_r^2\pi^2 C_F^2}{nm_1m_2} \left\{ \frac{1-\delta_{l0}}{l(l+1)(2l+1)} \left(D_s + \left(1 + \frac{m_1m_2}{2m_r^2} \right) X_{LS} \right) + \frac{8\delta_{l0}}{3} \mathcal{S}_{12} \right\} \\ + \frac{m_r^2\pi^2 C_F}{4n^2} \left\{ \frac{1}{m_1m_2} C_F + \frac{1}{m_r^2} \left[-3C_F + \frac{8n}{2l+1} \left(C_F + \frac{C_A}{2} \right) - 4nC_F\delta_{l0} \right] \right\}, \quad (\text{B5})$$

where, in comparison to Ref. [6], we express the results in the spin basis $\{\mathbf{S}, \mathbf{S}^-\}$:

$$\mathcal{S}_{12} \equiv \langle \mathbf{S}_1 \cdot \mathbf{S}_2 \rangle = \frac{1}{2} (s(s+1) - s_1(s_1+1) - s_2(s_2+1)), \quad (\text{B6})$$

$$D_s \equiv \frac{1}{2} \langle S_{12}(\mathbf{r}) \rangle = \frac{2l(l+1)s(s+1) - 3X_{LS} - 6X_{LS}^2}{(2l-1)(2l+3)}, \quad (\text{B7})$$

$$X_{LS} \equiv \langle \mathbf{L} \cdot \mathbf{S} \rangle = \frac{1}{2} [j(j+1) - l(l+1) - s(s+1)], \quad (\text{B8})$$

and finally

$$c_3^{\text{nc}} = \pi^2 (C_F^3 \xi_{\text{FFF}}^{\text{SD}} + C_F^2 C_A (\xi_{\text{FFA}}^{\text{SD}} + \xi_{\text{FFA}}^{\text{SI}}) + C_F^2 T_F n_f (\xi_{\text{FFnf}}^{\text{SD}} + \xi_{\text{FFnf}}^{\text{SI}}) - \frac{n}{6} \beta_0 c_2^{\text{nc}} \\ + C_A^3 \xi_{\text{AAA}} + C_A^2 C_F \xi_{\text{AAF}} + C_A C_F T_F n_f \xi_{\text{AFnf}} + C_F^2 T_F \xi_{\text{FF}} + C_F^3 \xi_{\text{FFF}}^{\text{SI}}). \quad (\text{B9})$$

Again, in comparison to Ref. [6], we express the results in the spin basis $\{\mathbf{S}, \mathbf{S}^-\}$,

$$\xi_{\text{FFF}}^{\text{SD}} = \frac{1}{3n} \left\{ \frac{-3(1-\delta_{l0})}{l(l+1)(2l+1)} \left(\frac{2m_r^2}{m_1m_2} D_s + X_{LS} \right) - \frac{8m_r^2}{m_1m_2} \mathcal{S}_{12} \delta_{l0} \left[2 + 3 \frac{m_1m_2}{m_2^2 - m_1^2} \ln \left(\frac{m_1^2}{m_2^2} \right) \right] \right\}, \quad (\text{B10})$$

$$\xi_{\text{FFnf}}^{\text{SD}} = \frac{2m_r^2}{9n^2 m_1 m_2} \left\{ \frac{1-\delta_{l0}}{l(l+1)(2l+1)} \left[2n(4\mathcal{S}_{12} - D_s) + 6 \left(D_s + \left(1 + \frac{m_1m_2}{2m_r^2} \right) X_{LS} \right) \left(\frac{3n}{2l+1} + \frac{n}{2l(l+1)(2l+1)} + l + \frac{1}{2} \right) \right. \right. \\ \left. \left. + 2n \left\{ S_1(l+n) + S_1(2l-1) - 2S_1(2l+1) - l(\Sigma_1^{(k)} + \Sigma_1^{(m)}) + n\Sigma_b - \Sigma_1^{(m)} + \frac{1}{6} \right\} \right] \right. \\ \left. + 8\delta_{l0} \mathcal{S}_{12} \left[1 + 4n \left(\frac{11}{12} - \frac{1}{n} - S_1(n-1) - S_1(n) + nS_2(n) \right) \right] \right\}, \quad (\text{B11})$$

$$\xi_{\text{FFA}}^{\text{SD}} = \frac{m_r^2}{m_1 m_2} \left\{ \frac{1-\delta_{l0}}{l(l+1)(2l+1)n} \left[\frac{2}{3} \left(D_s + \left(1 + \frac{m_1m_2}{2m_r^2} \right) X_{LS} \right) \right. \right. \\ \left. \left. \times \left\{ 22S_1(2l+1) - 17S_1(l+n) - 5S_1(2l-1) + 11[l(\Sigma_1^{(k)} + \Sigma_1^{(m)}) - n\Sigma_b + \Sigma_1^{(m)}] \right. \right. \right. \\ \left. \left. - \frac{5(2l+1)}{4n} - \frac{15}{2(2l+1)} - \frac{5}{4(l(l+1)(2l+1))} + \frac{1}{6} + \frac{3}{2} \ln \left(\frac{m_1m_2}{4m_r^2} \right) + 3L_H \right\} - \frac{2}{9} (2D_s + \mathcal{S}_{12}) \right. \\ \left. - 2X_{LS} \left(2(S_1(2l-1) - S_1(l+n)) + \frac{2l+1}{2n} + \frac{1}{2(l(l+1)(2l+1))} + \frac{3}{2l+1} - 2 + \frac{m_1^2 - m_2^2}{4m_1m_2} \ln \frac{m_1}{m_2} + \frac{1}{2} \ln \left(\frac{m_1m_2}{4m_r^2} \right) + L_H \right) \right. \\ \left. - \frac{4\delta_{l0}\mathcal{S}_{12}}{3n} \left[-\frac{67}{3} S_1(l+n) - 7L_H + \frac{65S_1(n)}{3} + \frac{44n\Sigma_2^{(k)}}{3} + \frac{1}{6n} + \frac{41}{18} \right. \right. \\ \left. \left. + \frac{1}{m_1 - m_2} \left((5m_2 - 2m_1) \ln \left(\frac{m_1}{2m_r} \right) - (5m_1 - 2m_2) \ln \left(\frac{m_2}{2m_r} \right) \right) \right] \right\}, \quad (\text{B12})$$

where $L_H = \ln\left(\frac{n}{C_F\alpha_s}\right) + S_1(n+l)$. The various $\Sigma_1, \Sigma_b, \dots$, above are finite sum functions, which are defined in Appendix I of Ref. [6].

The other color functions ξ_X^{SI} in Eq. (B9) are not affected by the change of spin basis, and can be found in Eqs. (I.15)–(I.21) of Ref. [6].

The case of equal masses is recovered by taking the limit $m = m_1 = m_2$ in all the color functions involved in Eq. (B9), except for ξ_{FF} (Eq. (I.18) in Ref. [6]), where we shall add the annihilation diagrams and, for equal masses, we obtain instead:

$$\xi_{\text{FF}} = \frac{\delta_{l0}}{n} \left(-2S_{12} + \left(2S_{12} - \frac{1}{2} \right) \ln(2) + \frac{19}{30} \right). \quad (\text{B13})$$

Finally, we would like to mention that we can check that the spectrum produced by the potentials obtained in different matching schemes is equal. Indeed, this check gives a nontrivial relation among some finite sums that, even though we did not prove it explicitly, holds true for any arbitrary set of quantum numbers we tried:

$$S_1(2l) + S_1(1+2l) - 2S_1(l+n) + 2l\Sigma_1^{(k)}(n, l) + 2(l+1)\Sigma_1^{(m)}(n, l) = 1. \quad (\text{B14})$$

APPENDIX C: THE N³LL HEAVY QUARKONIUM SPECTRUM

After adding the ultrasoft and soft/hard running to the N³LO result, one obtains the N³LL P -wave spectrum. It reads

$$E_{\text{N}^3\text{LL}}(n, l, s, j) = E_n^C \left(1 + \frac{\alpha_s}{\pi} \tilde{P}_1(L_\nu) + \left(\frac{\alpha_s}{\pi} \right)^2 \tilde{P}_2(L_\nu) + \left(\frac{\alpha_s}{\pi} \right)^3 \tilde{P}_3(L_\nu) \right), \quad (\text{C1})$$

$$\tilde{P}_1(L_\nu) = P_1(L_\nu) = \beta_0 L_\nu + \frac{a_1}{2}, \quad (\text{C2})$$

$$\tilde{P}_2(L_\nu) = \frac{3}{4} \beta_0^2 L_\nu^2 + \left(-\frac{\beta_0^2}{2} + \frac{\beta_1}{4} + \frac{3\beta_0 a_1}{4} \right) L_\nu + \tilde{c}_2, \quad (\text{C3})$$

$$\begin{aligned} \tilde{P}_3(L_\nu) = & \frac{1}{2} \beta_0^3 L_\nu^3 + \left(-\frac{7\beta_0^3}{8} + \frac{7\beta_0\beta_1}{16} + \frac{3}{4} \beta_0^2 a_1 \right) L_\nu^2 \\ & + \left(\frac{\beta_0^3}{4} - \frac{\beta_0\beta_1}{4} + \frac{\beta_2}{16} - \frac{3}{8} \beta_0^2 a_1 + 2\beta_0 \tilde{c}_2 + \frac{3\beta_1 a_1}{16} \right) L_\nu \\ & + \tilde{c}_3. \end{aligned} \quad (\text{C4})$$

The coefficients $\tilde{c}_i = \tilde{c}_i^c + \tilde{c}_i^{\text{nc}}$ are split into contributions from the static potential and those including the relativistic corrections.

\tilde{c}_i^c only get contributions from the resummation of the ultrasoft logarithms:

$$\tilde{c}_2^c = c_2^c + \delta c_2^c, \quad (\text{C5})$$

$$\tilde{c}_3^c = c_3^c + \delta c_3^c, \quad (\text{C6})$$

where $c_{2,3}^c$ are the coefficients computed for the fixed-order spectrum in Eqs. (147) and (150) in Ref. [5] for (un)equal masses, and $\delta c_{2,3}^c$

$$\delta c_2^c = -\frac{\pi C_A^3}{6} \frac{2\pi}{\beta_0} \ln \frac{\alpha_{\text{us}}}{\alpha_s}, \quad (\text{C7})$$

$$\begin{aligned} \delta c_3^c = & \frac{\pi C_A^3}{32} \left[\frac{8}{3} \frac{2\pi}{\beta_0} \ln \frac{\alpha_{\text{us}}}{\alpha_s} (\beta_0 - 2a_1) \right. \\ & - 8\pi^2 \frac{2\pi}{\beta_0} \frac{\alpha_{\text{us}} - \alpha_s}{\alpha_s} \\ & \left. \times \left(\frac{8\beta_1}{3\beta_0} \frac{1}{(4\pi)^2} - \frac{1}{27\pi^2} (C_A(47 + 6\pi^2) - 10T_f n_f) \right) \right]. \end{aligned} \quad (\text{C8})$$

\tilde{c}_i^{nc} get contributions from the ultrasoft resummation, from the hard resummation, and from the difference of evaluating the ultrasoft energy at the ultrasoft scale (which is included in the ultrasoft part of the coefficients), i.e.,

$$\tilde{c}_2^{\text{nc}} = c_2^{\text{nc}} + \delta c_2^{\text{nc}}, \quad (\text{C9})$$

$$\tilde{c}_3^{\text{nc}} = c_3^{\text{nc}} + \delta c_3^{\text{nc}}, \quad (\text{C10})$$

where $c_{2,3}^{\text{nc}}$ are the coefficients presented in the previous section and computed for the fixed-order spectrum in (Ref. [6]) Ref. [5] for (un)equal masses, and

$$\delta c_2^{\text{nc}} = \delta c_2^{\text{nc,h}} + \delta c_2^{\text{nc,us}}, \quad (\text{C11})$$

$$\delta c_3^{\text{nc}} = \delta c_3^{\text{nc,h}} + \delta c_3^{\text{nc,us}} \quad (\text{C12})$$

where

$$\delta c_2^{\text{nc,us}} = \frac{2\pi C_A C_F}{3n^2} \left(C_F - \frac{2n}{2l+1} (C_A + 4C_F) \right) \frac{2\pi}{\beta_0} \ln \frac{\alpha_{\text{us}}}{\alpha_s}, \quad (\text{C13})$$

$$\begin{aligned}
\delta c_3^{\text{nc.us}} = & \frac{2\pi}{\beta_0} \frac{\alpha_{\text{us}} - \alpha_s}{\alpha_s} \left[\frac{\pi\beta_0}{3} \left(\frac{C_A^3}{4} \left(L_{\text{us}} - \frac{5}{6} \right) - C_F^3 L_n^E \right) + \pi^3 C_A C_F \left(\frac{2C_A}{(2l+1)n} + C_F \left(\frac{8}{(2l+1)n} - \frac{1}{n^2} \right) \right) \right. \\
& \times \left. \left(\frac{8\beta_1}{3\beta_0} \frac{1}{(4\pi)^2} - \frac{1}{27\pi^2} (C_A(47+6\pi^2) - 10T_f n_f) + \frac{\beta_0}{3\pi^2} \left(L_{\text{us}} - \frac{5}{6} \right) \right) \right] \\
& + \frac{\pi C_F}{3n^2} \frac{2\pi}{\beta_0} \ln \frac{\alpha_{\text{us}}}{\alpha_s} \left[C_F(C_A - 2C_F)\beta_0 \frac{n(1-\delta_{l0})}{l(l+1)(2l+1)} + 2C_A a_1 \left(C_F - \frac{2n}{2l+1} (C_A + 4C_F) \right) \right. \\
& - C_A \beta_0 \left(C_F - \frac{4n}{(2l+1)^2} (C_A + C_F(7+6l)) + \frac{4n^2}{2l+1} (C_A + 4C_F) \left(\Sigma_b(n, l) - \frac{\pi^2}{6} \right) \right) \left. \right] \\
& - \frac{\pi^2}{3} \left[\frac{C_A^3}{2} + \frac{4C_A^2 C_F}{(2l+1)n} + 2C_A C_F^2 \left(\frac{8}{(2l+1)n} - \frac{1}{n^2} \right) \right] \left(\frac{\alpha_{\text{us}}}{\alpha_s} L_{\nu_{\text{us}}} - L_\nu \right), \tag{C14}
\end{aligned}$$

where we have omitted the contribution of $\langle \text{reg} \frac{1}{\vec{r}} \rangle$ to the S -wave spectrum.

The NNLL hard contribution of the spectrum coefficients is known for general quantum numbers,

$$\begin{aligned}
\delta c_2^{\text{nc.h}} = & -\frac{2\pi^2 C_F^2 (1-\delta_{l0})}{n(2l+1)l(l+1)} \frac{m_r^2}{m_1 m_2} \left\{ \delta [c_F^{(1)} c_F^{(2)}] D_s + X_{LS} \left(\delta c_F^{(2)} + \delta c_F^{(1)} + \frac{\delta c_S^{(1)} m_2}{2m_1} + \frac{\delta c_S^{(2)} m_1}{2m_2} \right) \right\} \\
= & \frac{2\pi^2 C_F^2 (1-\delta_{l0})}{n(2l+1)l(l+1)} \left(1 - z^{-\frac{\gamma_0}{2}} \right) \left(X_{LS} + \frac{m_r^2}{m_1 m_2} \left(1 + z^{-\frac{\gamma_0}{2}} \right) D_s \right), \tag{C15}
\end{aligned}$$

where we have defined

$$\delta c_F^{(i)} = c_F^{(i)}(\nu_h, \nu) - c_F^{(i)}(\nu, \nu), \tag{C16}$$

$$\delta c_S^{(i)} = c_S^{(i)}(\nu_h, \nu) - c_S^{(i)}(\nu, \nu) = 2(c_F^{(i)}(\nu_h, \nu) - c_F^{(i)}(\nu, \nu)), \tag{C17}$$

$$\delta [c_F^{(1)} c_F^{(2)}] = c_F^{(1)}(\nu_h, \nu) c_F^{(2)}(\nu_h, \nu) - c_F^{(1)}(\nu, \nu) c_F^{(2)}(\nu, \nu) \tag{C18}$$

and truncated to the appropriate order.

Finally, the third-order hard coefficient is obtained from all the relativistic potentials except for V_r and V_{S^2} , from which we only obtain the P -wave contribution. We split it into a spin-dependent and a spin-independent piece,

$$\delta c_3^{\text{nc.h}} = \delta c_3^{\text{SI,h}} + \delta c_3^{\text{SD,h}} \tag{C19}$$

where

$$\begin{aligned}
\delta c_3^{\text{SD,h}} = & \frac{2\pi^2 C_F^2 (1-\delta_{l0})}{n(2l+1)l(l+1)} \frac{m_r^2}{m_1 m_2} \left\{ \left[\beta_0 \left(S_1(l+n) + \frac{4n-(2l+1)}{4n} - \frac{1}{2} (S_1(2l-1) + S_1(2l+2)) \right) + l \Sigma_1^{(k)} \right. \right. \\
& + l \Sigma_1^{(m)} - n \Sigma_2^{(k)} - n \Sigma_2^{(m)} + \frac{\pi^2 n}{6} + \Sigma_1^{(m)} \left. \right] - \frac{3a_1}{4} \left[X_{LS} \left(\delta c_F^{(1)} + \delta c_F^{(2)} + \frac{\delta c_S^{(1)} m_2}{2m_1} + \frac{\delta c_S^{(2)} m_1}{2m_2} \right) + \delta [c_F^{(1)} c_F^{(2)}] D_s \right] \\
& + \frac{1}{12} (\beta_0 + 8C_A) X_{LS} \left((\delta c_F^{(1)} + \delta c_F^{(2)}) + \frac{\delta c_S^{(1)} m_2}{2m_1} + \frac{\delta c_S^{(2)} m_1}{2m_2} \right) - \frac{\delta [c_F^{(1)} c_F^{(2)}] D_s}{12} (2C_A - 3\beta_0) \\
& - C_A \left(2S_1(l+n) + \frac{2n-(2l+1)}{2n} - S_1(2l-1) - S_1(2l+2) \right) \\
& \times \left. \left[\delta [c_F^{(1)} c_F^{(2)}] D_s + X_{LS} \left(\frac{\delta c_F^{(1)} m_2}{2m_r} + \frac{\delta c_F^{(2)} m_1}{2m_r} \right) \right] + \frac{1}{3} \delta [c_F^{(1)} c_F^{(2)}] \mathcal{S}_{12} (7C_A - 2\beta_0) \right\} \tag{C20}
\end{aligned}$$

$$\begin{aligned}
&= \frac{2\pi^2 C_F^2 (1 - \delta_{l0}) m_r^2}{l(l+1)(2l+1)nm_1 m_2} (1 - z^{-C_A}) \left\{ \left(D_s(z^{-C_A} + 1) + \frac{m_1 m_2}{m_r^2} X_{LS} \right) \right. \\
&\times \left[\beta_0 \left(-l \Sigma_1^{(k)}(n, l) - (l+1) \Sigma_1^{(m)}(n, l) + n(\Sigma_2^{(k)}(n, l) + \Sigma_2^{(m)}(n, l)) - \frac{\pi^2 n}{6} - 1 \right) \right. \\
&+ a_1 + \frac{z^{-\beta_0 - \frac{\gamma_0}{2}} - 1}{z^{-\frac{\gamma_0}{2}} - 1} \frac{C_A + C_F}{2} - \frac{z^{-\beta_0 - C_A} - 1}{z^{-C_A} - 1} \frac{C_A L_H}{2} + \frac{\beta_0 - C_A}{2} \left(\frac{2l+1}{2n} - 2S_1(l+n) + S_1(2l-1) + S_1(2l+2) - 1 \right) \left. \right] \\
&+ \frac{1}{2} D_s(z^{-C_A} + 1) \left[-\frac{\beta_0}{3} + \frac{z^{-\beta_0 - C_A} + 1}{z^{-C_A} + 1} (C_A + C_F) - C_A \left(\frac{2l+1}{2n} - \frac{8}{3} - 2S_1(l+n) + S_1(2l-1) + S_1(2l+2) \right) \right. \\
&+ \left. \frac{z^{-\beta_0 - C_A} + 1}{z^{-C_A} + 1} L_H + \frac{(z^{-\beta_0 - 2C_A} - 1)}{z^{-2C_A} - 1} \ln \frac{m_1 m_2}{4m_r^2} \right] + \frac{z^{-C_A}}{2(z^{-C_A} - 1)} \frac{\alpha_h - \alpha_s}{\alpha_s} \left(\frac{\gamma_1}{2\beta_0} - \frac{\beta_1 C_A}{\beta_0^2} \right) \left(D_s z^{-C_A} + \frac{m_1 m_2}{2m_r^2} X_{LS} \right) \\
&- \frac{C_A (z^{-\beta_0 - C_A} - 1)}{z^{-C_A} - 1} X_{LS} \left(\frac{m_2}{2m_r} \ln \frac{m_1}{2m_r} + \frac{m_1}{2m_r} \ln \frac{m_2}{2m_r} \right) + \frac{4}{3} S_{12} \left(\frac{\beta_0}{2} - \frac{7C_A}{4} \right) (z^{-C_A} + 1) \left. \right\} \\
&- \frac{2\pi^2 C_A C_F^2 (1 - \delta_{l0}) z^{-\frac{\gamma_0}{2}}}{(l(l+1)(2l+1)n)} \frac{m_r}{m_1 m_2} \left(D_s m_r z^{-\frac{\gamma_0}{2}} + \frac{m_1 m_2}{2m_r} X_{LS} \right) \left(\frac{\alpha_h}{\alpha_s} L_{\nu_h} - L_\nu \right), \tag{C21}
\end{aligned}$$

$$\delta c_3^{\text{SI,h}} = \frac{\pi^2 C_F^2 (1 - \delta_{l0})}{n(2l+1)l(l+1)} \frac{m_r^2}{m_1 m_2} \left\{ \left[\frac{m_1}{m_2} + \frac{m_2}{m_1} \right] \left[-\frac{5}{12} C_A (z^{-2C_A} - 1) + \frac{1}{3} T_f n_f \left(z^{-2C_A} - 1 + \left(\frac{20}{13} + \frac{32 C_F}{13 C_A} \right) [1 - z^{-\frac{13C_A}{6}}] \right) \right] \right\}. \tag{C22}$$

-
- [1] A. Billoire, *Phys. Lett.* **92B**, 343 (1980).
[2] A. Pineda and F. J. Yndurain, *Phys. Rev. D* **58**, 094022 (1998).
[3] N. Brambilla, A. Pineda, J. Soto, and A. Vairo, *Phys. Lett. B* **470**, 215 (1999).
[4] Y. Kiyo and Y. Sumino, *Phys. Lett. B* **730**, 76 (2014).
[5] Y. Kiyo and Y. Sumino, *Nucl. Phys.* **B889**, 156 (2014).
[6] C. Peset, A. Pineda, and M. Stahlhofen, *J. High Energy Phys.* **05** (2016) 017.
[7] N. Brambilla and A. Vairo, *Phys. Rev. D* **71**, 034020 (2005).
[8] S. Titard and F. J. Yndurain, *Phys. Rev. D* **51**, 6348 (1995).
[9] A. Pineda, *Phys. Rev. D* **84**, 014012 (2011).
[10] A. Pineda and J. Soto, *Nucl. Phys. B, Proc. Suppl.* **64**, 428 (1998).
[11] N. Brambilla, A. Pineda, J. Soto, and A. Vairo, *Nucl. Phys.* **B566**, 275 (2000).
[12] N. Brambilla, A. Pineda, J. Soto, and A. Vairo, *Rev. Mod. Phys.* **77**, 1423 (2005).
[13] A. Pineda, *Prog. Part. Nucl. Phys.* **67** (2012) 735.
[14] A. Pineda, Heavy quarkonium and nonrelativistic effective field theories, Ph.D. thesis, Barcelona University, 1998.
[15] A. H. Hoang, M. C. Smith, T. Stelzer, and S. Willenbrock, *Phys. Rev. D* **59**, 114014 (1999).
[16] M. Beneke, *Phys. Lett. B* **434**, 115 (1998).
[17] I. I. Y. Bigi, M. A. Shifman, N. G. Uraltsev, and A. I. Vainshtein, *Phys. Rev. D* **50**, 2234 (1994).
[18] A. Pineda, *J. High Energy Phys.* **06** (2001) 022.
[19] A. H. Hoang, A. Jain, I. Scimemi, and I. W. Stewart, *Phys. Rev. D* **82**, 011501 (2010).
[20] N. Brambilla, J. Komijani, A. S. Kronfeld, and A. Vairo (TUMQCD Collaboration), *Phys. Rev. D* **97**, 034503 (2018).
[21] N. Brambilla, Y. Sumino, and A. Vairo, *Phys. Lett. B* **513**, 381 (2001).
[22] N. Brambilla, Y. Sumino, and A. Vairo, *Phys. Rev. D* **65**, 034001 (2002).
[23] S. Recksiegel and Y. Sumino, *Phys. Rev. D* **67**, 014004 (2003).
[24] S. Recksiegel and Y. Sumino, *Phys. Lett. B* **578**, 369 (2004).
[25] A. H. Hoang, Z. Ligeti, and A. V. Manohar, *Phys. Rev. Lett.* **82**, 277 (1999).
[26] V. Mateu and P. G. Ortega, *J. High Energy Phys.* **01** (2018) 122.
[27] A. Pineda and J. Segovia, *Phys. Rev. D* **87**, 074024 (2013).
[28] Y. Kiyo, A. Pineda, and A. Signer, *Nucl. Phys.* **B841**, 231 (2010).
[29] C. Peset, A. Pineda, and J. Segovia, *J. High Energy Phys.* **09** (2018) 167.
[30] W. E. Caswell and G. P. Lepage, *Phys. Lett.* **167B**, 437 (1986).
[31] G. T. Bodwin, E. Braaten, and G. P. Lepage, *Phys. Rev. D* **51**, 1125 (1995); **55**, 5853 (1997).
[32] M. E. Luke, A. V. Manohar, and I. Z. Rothstein, *Phys. Rev. D* **61**, 074025 (2000).

- [33] A. H. Hoang and M. Stahlhofen, *Phys. Rev. D* **75** (2007) 054025.
- [34] A. H. Hoang and M. Stahlhofen, *J. High Energy Phys.* **06** (2011) 088.
- [35] A. Pineda and J. Soto, *Phys. Lett. B* **495**, 323 (2000).
- [36] N. Brambilla, A. Vairo, X. G. i Tormo, and J. Soto, *Phys. Rev. D* **80**, 034016 (2009).
- [37] A. Pineda and M. Stahlhofen, *Phys. Rev. D* **84**, 034016 (2011).
- [38] A. Pineda, *Phys. Rev. D* **65**, 074007 (2002).
- [39] B. A. Kniehl, A. A. Penin, A. Pineda, V. A. Smirnov, and M. Steinhauser, *Phys. Rev. Lett.* **92**, 242001 (2004); **104**, 199901(E) (2010).
- [40] A. A. Penin, A. Pineda, V. A. Smirnov, and M. Steinhauser, *Phys. Lett. B* **593**, 124 (2004); **677**, 343(E) (2009).
- [41] A. V. Manohar, *Phys. Rev. D* **56**, 230 (1997).
- [42] G. Amoros, M. Beneke, and M. Neubert, *Phys. Lett. B* **401**, 81 (1997).
- [43] A. Czarnecki and A. G. Grozin, *Phys. Lett. B* **405**, 142 (1997); **650**, 447(E) (2007).
- [44] S. N. Gupta and S. F. Radford, *Phys. Rev. D* **24**, 2309 (1981).
- [45] W. Buchmuller, Y. J. Ng, and S. H. H. Tye, *Phys. Rev. D* **24** (1981) 3003.
- [46] J. T. Pantaleone, S. H. H. Tye, and Y. J. Ng, *Phys. Rev. D* **33** (1986) 777.
- [47] Y. Q. Chen, Y. P. Kuang, and R. J. Oakes, *Phys. Rev. D* **52**, 264 (1995).
- [48] M. E. Luke and A. V. Manohar, *Phys. Lett. B* **286**, 348 (1992).
- [49] C. W. Bauer and A. V. Manohar, *Phys. Rev. D* **57**, 337 (1998).
- [50] B. Blok, J. G. Korner, D. Pirjol, and J. C. Rojas, *Nucl. Phys.* **B496**, 358 (1997).
- [51] A. Pineda, *Phys. Rev. D* **55**, 407 (1997); **59**, 099901(E) (1999).
- [52] A. Krämer, H. G. Dosch, and R. A. Bertlmann, *Phys. Lett. B* **223**, 105 (1989); *Fortschr. Phys.* **40**, 93 (1992); Voloshin, *Sov. J. Nucl. Phys.* **35**, 592 (1982); M. Campostrini, A. Di Giacomo, and S. Olejnik, *Z. Phys. C* **31**, 577 (1986); G. Curci, A. Di Giacomo, and G. Paffuti, *Z. Phys. C* **18**, 135 (1983).
- [53] R. F. Lebed and E. S. Swanson, *Phys. Rev. D* **96**, 056015 (2017).
- [54] C. Patrignani *et al.* (Particle Data Group), *Chin. Phys. C* **40**, 100001 (2016).
- [55] A. Pineda, *J. Phys. G* **29**, 371 (2003).
- [56] B. A. Kniehl, A. A. Penin, M. Steinhauser, and V. A. Smirnov, *Phys. Rev. D* **65**, 091503 (2002).
- [57] G. S. Bali, K. Schilling, and A. Wachter, *Phys. Rev. D* **56**, 2566 (1997).
- [58] Y. Koma and M. Koma, *Nucl. Phys.* **B769**, 79 (2007).
- [59] W. Fischler, *Nucl. Phys.* **B129**, 157 (1977).
- [60] Y. Schröder, *Phys. Lett. B* **447**, 321 (1999).
- [61] M. Peter, *Phys. Rev. Lett.* **78**, 602 (1997).
- [62] N. Brambilla, A. Pineda, J. Soto, and A. Vairo, *Phys. Rev. D* **60**, 091502 (1999).
- [63] A. V. Smirnov, V. A. Smirnov, and M. Steinhauser, *Phys. Lett. B* **668**, 293 (2008).
- [64] C. Anzai, Y. Kiyo, and Y. Sumino, *Phys. Rev. Lett.* **104**, 112003 (2010).
- [65] A. V. Smirnov, V. A. Smirnov, and M. Steinhauser, *Phys. Rev. Lett.* **104**, 112002 (2010).
- [66] B. A. Kniehl, A. A. Penin, V. A. Smirnov, and M. Steinhauser, *Nucl. Phys.* **B635**, 357 (2002).
- [67] S. N. Gupta and S. F. Radford, *Phys. Rev. D* **25**, 3430 (1982).